OPTICAL AND DIELECTRIC PROPERTIES OF LIQUID CRYSTALS AND LIQUID CRYSTAL NANOCOMPOSITES

PROJECT REPORT

Submitted by

UMA MAHESWARI. P

Register No: 091505100011

in partial fulfillment for the award of the degree

of

MASTER OF TECHNOLOGY

in

NANOTECHNOLOGY

ANNA UNNIVESITY OF TECHNOLOGY COIMBATORE

COIMBATORE- 641047.

MAY-2011

ANNA UNNIVESITY OF TECHNOLOGY COIMBATORE

COIMBATORE- 641047

Department of Nanotechnology

PROJECT WORK

PHASE II

MAY 2011

This is to certify that the project entitled

OPTICAL AND DIELECTRIC PROPERTIES OF LIQUID CRYSTALS AND LIQUID CRYSTAL NANOCOMPOSITES

is the bonafide report of project work done by

UMA MAHESWARI. P

Register No: 091505100011

of M.Tech(Nanotechnology) during the year 2010-2011.

---------- ----------

Project Internal Guide Head of the Department

Dr. K. Rajasekar **Dr.P. Renuka Devi**

Submitted for the Project Viva-Voce examination held on----------

---------- ----------

Internal Examiner External Examiner

CERTIFICATE

This is to certify that Ms P.Uma Maheswari a student of Master of Technology in Nanotechnology, Anna University of Technology, Coimbatore has carried out the research project titled "Optical and Dielectric properties of Liquid Crystals and Liquid Crystal Nanocomposites" under my supervision at the Soft Condensed Matter Lab, Raman Research Institute, Bangalore during the period 15 November 2010 to 15 May 2011 as partial fulfillment for the award of Master of Technology.

19 May 2011

R Pratibha

Associate Professor
Soft Condensed matter Lab
Raman Research Institute
Sadashivanagar
Bangalore -560080
India

DECLARATION

I affirm that the project work titled **"Optical and Dielectric properties of Liquid Crystals and Liquid Crystal Nanocomposites"** being submitted in partial fulfillment for the award of "**Master of Technology"** is the original work carried out by me. It has not formed the part of any other project work submitted for a award of any degree or diploma, either in this or any other University.

Uma Maheswari. P

091505100011

I certify that the declaration made above by the candidate is true

Dr. K. Rajasekar,

Assistant Professor,

Anna University of Technology,

Coimbatore.

ACKNOWLEDGEMENT

First and foremost I express special and my hearty thanks to **Dr. R. Pratibha,** Associate Professor, Soft Condensed Matter Lab, Raman Research Institute, Bangalore, for her guidance, support and kind help throughout my project.

I thank to **Dr. Reji Philip,** Associate Professor, Light and Matter Physics, Raman Research Institute, Bangalore for his kind help in Non Linear Optics analysis.

I express my deep gratitude and sincere thanks to **Dr. K. Rajasekar,** Assistant Professor, Department of Nanotechnology, Coimbatore for his expert guidance, suggestions and active encouragement for the fulfillment of the project work.

I also wish to thank **Dr. P. Renuka Devi,** Head of the Department, Department of Nanotechnology, Anna University of Technology, Coimbatore whole heartedly for her support and inspiration.

I thank **Dr. K. Karunakaran,** Vice Chancellor, Anna University of Technology, Coimbatore for his support to the students.

I express my deep gratitude towards our respected Dean Academics, **Dr.M.Saravanakumar**, Anna University of Technology, for his continuous encouragement and support.

I thank my RRI friends **Mrs. K.N. Vasudha, Mr B.S. Avinash, Mr. Smijesh, Mr. Safakath, Mr. Swaminathan, Mrs. Radhika, Ms.Monica, Mr. Sagar** and all in **RRI**, **Bangalore** who all are helped me in my project work.

I also thank **Mr.R. Rajesh, Mr. E. Hemanath, Mrs.K.G. Dhanalakshmi, Ms. Lavanya Priya, Mr. Saravana kumar, Mr. Chinna,** Research scholars, Dept. of Nanotechnology for their kind help throughout my course.

Last but not the least; I thank my **parents, brother, my dear friends** and others who helped me anonymously in completing this project successfully.

Uma Maheswari. P

CONTENTS

ABSTRACT

Composite materials with tunable optical properties are of great interest today because of the possible opto-electronic applications. Combination of two different materials both of which possess tunable properties would be very useful in forming such composites. It is well known that properties of nanoparticles depend on their shape, size and dielectric properties of the surrounding medium. Metal nanoparticles like gold and silver nanoparticles also exhibit the phenomenon of surface plasmon resonance which arises due to the collective oscillation of the conduction electrons. This results in a strong absorption band in the visible region. On the other hand liquid crystals possess various interesting temperature dependent physical properties like birefringence and also respond to electric fields. Interaction between nanomaterials and liquid crystals can therefore lead to changes in optical properties which can be tuned. Further liquid crystals which are characterized by order and fluidity also aid in obtaining periodic arrangements of the nanoparticles thus avoiding elaborate fabrication processes.

For the present study nanoparticles of different shapes were synthesized. The particles were characterized by absorption spectroscopy and TEM. Various liquid crystals-nanoparticle composites were prepared and characterized by polarising microscopy and dielectric spectroscopy. Finally the changes in the properties of the sample were noted using comparative studies.

LIST OF TABLES

LIST OF FIGURES

LIST OF SYMBOLS

S	Order parameter
Δn	Refractive index
n_e	Extraordinary refractive index
n_o	Ordinary refractive index
$\sigma_{\parallel}$	Conductivity parallel to the director
$\sigma_{\perp}$	Conductivity perpendicular to the director
K	Elastic constant
ε_o	Permittivity of free space
$\varepsilon_{\parallel}$	Dielectric permittivity parallel to the director
$\varepsilon_{\perp}$	Dielectric permittivity perpendicular to the director
$\Delta\varepsilon$	Dielectric anisotropy
$\varepsilon^{\prime}$	Real part of dielectric permittivity
$\varepsilon^{\prime\prime}$	Imaginary part of dielectric permittivity
γ	Extinction coefficient
σ_{ext}	Extinction cross section
β	Two photon absorption coefficient
I_o	Peak intensity
I_s	Saturation intensity
λ_m	Wavelength of m^{th} fringe
λ_n	Wavelength of n^{th} fringe
K_{11}	Splay elastic constant
V_{th}	Threshold voltage

LIST OF ABBREVIATIONS

LC	Liquid crystals
TLC	Thermotropic Liquid Crystals
5CB	4-cyano- 4’-pentylbiphenyl
PAA	Para- azoxyanisole
DDA	Discrete Dipole Approximation
TOAB	TetraOctylAmmonium Bromide
CTAB	CetylTrimethyl Ammonium Bromide
ITO	Indium Tin Oxide
I	Isotropic phase
N	Nematic phase
NLC	Nematic Liquid Crystal
DLC	Discotic Liquid Crystal
GNP	Gold NanoPantagons
$AgNO_3$	Silver Nitrate
NaOH	Sodium Hydroxide
TEM	Transmission Electron Microscopy
HRTEM	High Resolution Transmission Electron Microscopy

CHAPTER - I
INTRODUCTION

Nanotechnology, which is an upcoming and promising field deals with materials and devices obtained by the control of matter on the nanometer scale. In addition, nanoparticles can also be used to form composites, as such materials have the capacity to exhibit improved physical properties like enhanced optical, electrical and mechanical properties. These properties can also be tuned depending on the size and shape of the nano materials used in the composite. The ability to self-assemble metallic, magnetic and semiconducting nanoparticles into arrays, networks and circuits in a precise and controlled fashion is the key to fabrication of a variety of devices that make use of the intriguing properties of nanoscale materials. A variety of applications such as nanoscale electronics, functional coatings, optical memory and display devices are based on the collective properties of organized particles. Such applications require flexibility in controlling the architecture of the arrays. In this regard composite materials which can possess mechanical, electrical, thermal, optical, electrochemical, catalytic properties are very useful as the properties differ markedly from that of the individual components. In addition it would be even more useful if the materials forming the composites have tunable properties. One such combination of materials that are being studied extensively today are of liquid crystals (LCs) and nanoparticles (NPs). The reason for using liquid crystals is because they are partially ordered anisotropic fluids and have the property of self assembly. On the other hand noble metal nanoparticles exhibit properties like strong surface plasmon resonance because of the collective oscillation of conduction electrons (1). This is associated with a strong absorption band in the visible region. Therefore dispersion of such nanoparticles in liquid crystals can give rise to the tuning of the optical properties of the composite.

1.1 PRESENT WORK

The main motivation of this work was to study composites of liquid crystal with gold nanoparticles having different shapes. For this purpose gold nanoparticles having different shapes like pentagons of two different sizes and bipyramids were initially synthesised by simple chemical methods (20-23). The particles were characterized using several techniques like optical absorption and transmission electron microscopy. Composites of these particles were prepared

with a typical nematic liquid. After studying the composites by optical microscopy, various properties of the composites like optical absorbance, dielectric and elastic properties of were studied and compared with that of the pure liquid crystal. Non linear optical properties of some nanoparticles have also been measured.

1.2 LIQUID CRYSTALS

Liquid-crystal is a state of matter having properties in between the anisotropic solid and the isotropic liquid. The material properties possessed by them like optical, dielectric, elastic, magnetic properties are anisotropic in nature. Fig 1.1 shows the difference in the arrangement of the molecules in a solid, liquid crystal and liquid (2-5).

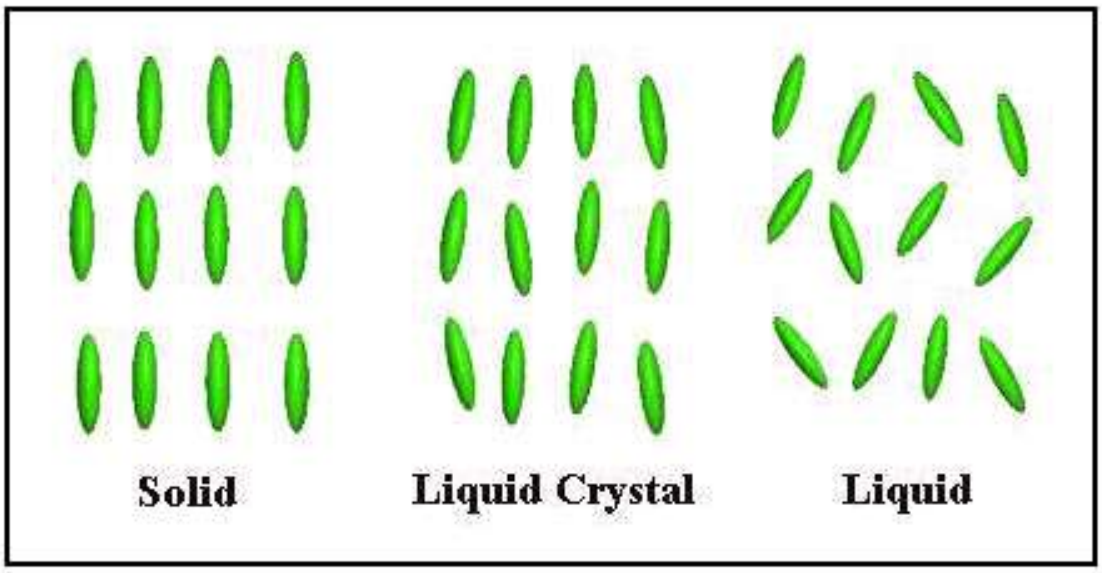

Fig 1.1: Molecular arrangement in the solid, liquid crystal and liquid phase.

The molecules in the liquid crystalline phases have some degree of orientational order and positional order. The average orientation direction of the molecules is called the director and is usually denoted by unit vector $\hat{n}$.

1.3 TYPES OF LIQUID CRYSTALS

Liquid crystals are classified into two main groups,

1. Thermotropic liquid crystals

2. Lyotropic liquid crystals.

In thermotropic liquid crystals (TLCs) the liquid crystalline or mesomorphic state is present as a function of temperature. TLCs are made up of a number of orientationally ordered mesophases obtained as function of temperature and are obtained on heating from the crystalline state. Lyotropic liquid crystals are formed by two or more components and exhibit liquid-crystalline properties in certain concentration ranges.

In the present work only thermotropic liquid crystals have been studied. These liquid crystals can be formed of different shaped molecules like rod-like, disc-like and bent-core molecules. In the present work thermotropic liquid crystals (TLCs) made of rod-like molecules have been studied in particular. We therefore describe some of the important properties of such liquid crystals.

The scheme of classification of liquid crystals and phases exhibited by the thermotropic liquid crystals made by rod like molecules is shown in Fig 1.2.

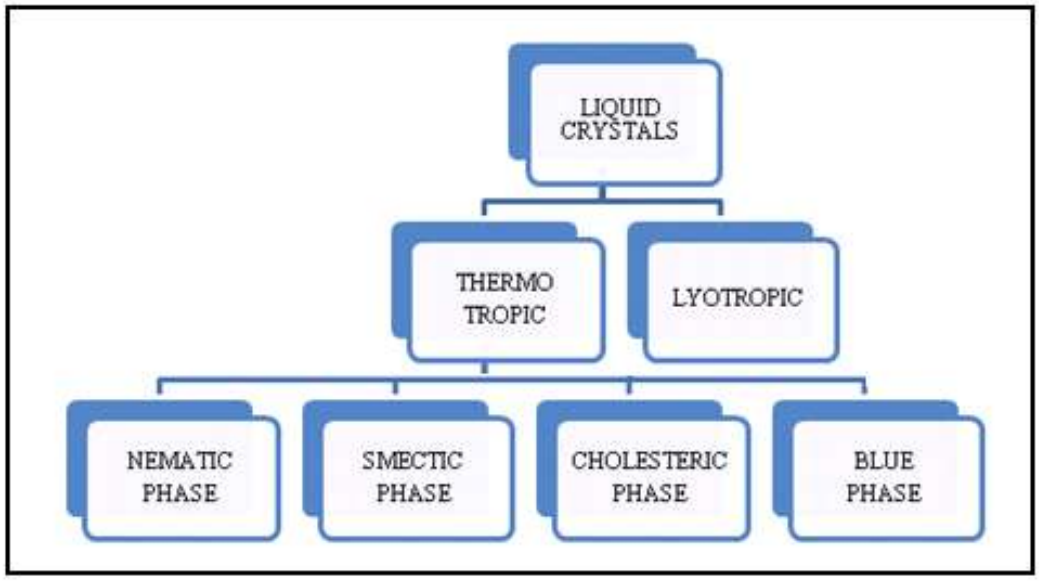

Fig 1.2: Classification of typical liquid crystals.

Typical examples of thermotropic liquid crystalline compounds are 4-Cyano-4'-pentylbiphenyl (5CB), Octyloxy cyanobiphenyl(8OCB).

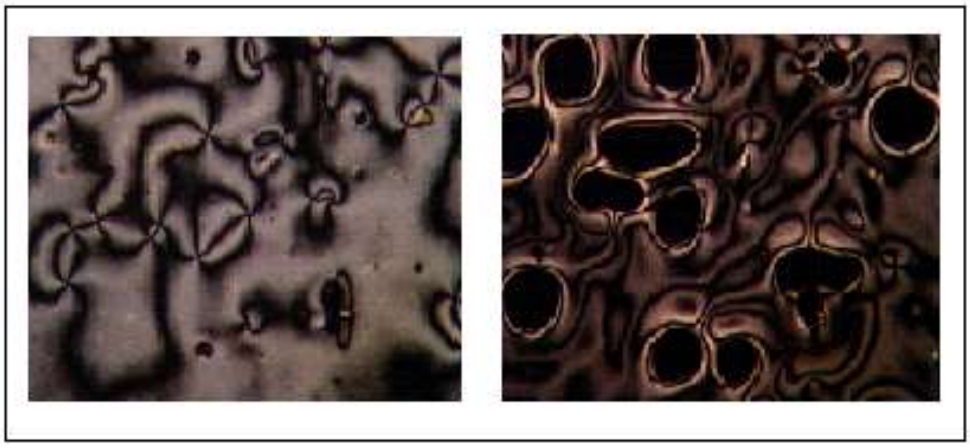

(a) Nematic phase(Room Tempreture) (b) Nematic- isotropic phase transition

Fig 1.3: The optical textures exhibited by 5CB.

TLCs can exhibit different phases in different temperature ranges. Some of the typical LC phases are nematic, smectic and cholesteric phases. The simplest type of LC phase is the nematic phase which is widely used in most practical devices.

1.4 NEMATIC PHASE

In the nematic phase the rod shaped molecules are oriented on the average along an axis called the director. The nematic phase has long range orientational order.

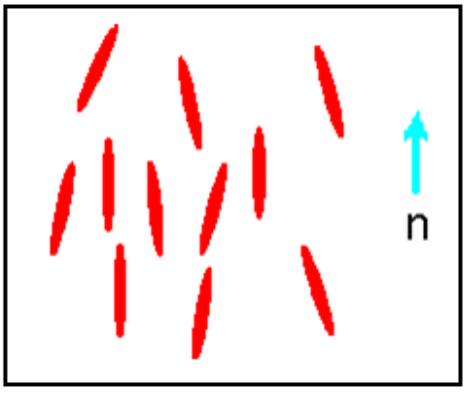

Fig 1.4 Molecular arrangements in the Nematic phase.

1.5 SMECTIC PHASE

In the smectic phases which are usually found at temperatures lower than the nematic phase a layered arrangement is present. The molecules are positionally ordered along one direction. They are different types of smectic phases S_A, S_C, and higher ordered smectic phases like S_B, S_F, S_I, S_E,. In the smectic A phase, the molecules are on an average along the layer normal and in the smectic C phase the average molecular direction makes an angle with the layer normal.

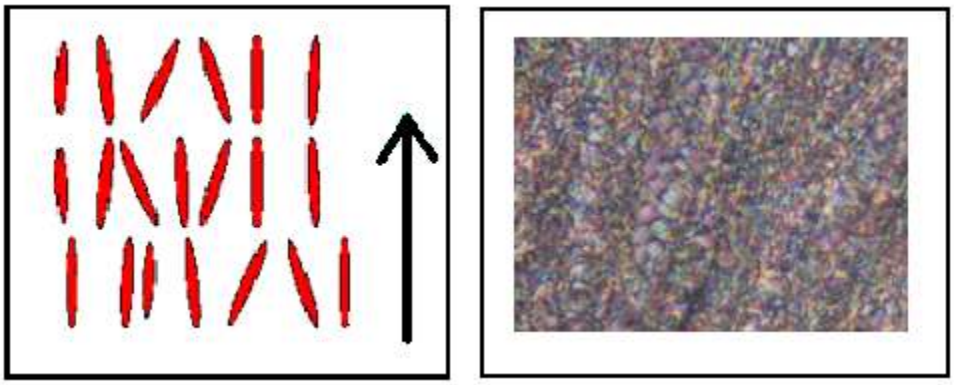

Fig 1.5: Molecular arrangement and optical texture of the Smectic A phase.

Fig 1.6: Molecular arrangements in the Smectic C phase.

1.6 CHOLESTERIC PHASE

Molecules which possess a chiral centre form this phase. In this phase the molecules twist along an axis which is orthogonal to the plane in which the director is present. The chiral pitch p refers to the distance over which the LC molecules undergo a twist of 180^0. The pitch typically changes when the temperature is altered or when other molecules are added to the LC host. This allows the pitch of a given material to be tuned.

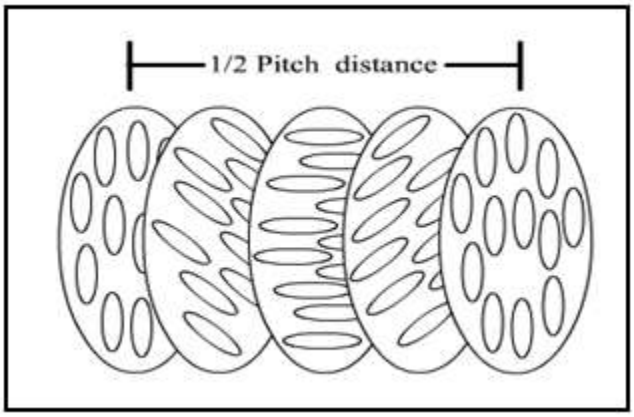

Fig 1.7: Molecular arrangement in the cholesteric phase.

As the present work is mainly on the nematic phase, some of the properties exhibited by nematic liquid crystals are described below.

1.7 ANISOTROPIC PHYSICAL PROPERTIES IN A LIQUID CRYSTAL

Order parameter

The order parameter is a measure of the distribution of these molecules about the director. A tensor order parameter is used to describe the orientational order of a liquid crystal. The order parameter is defined as

$$S = (1/2)\langle 3\cos^2\theta - 1 \rangle$$

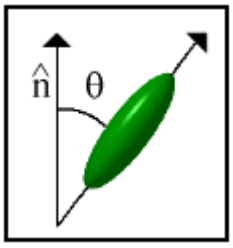

where θ is the angle between the LC molecular axis and the local director. The brackets denote both a temporal and spatial average. According to this definition for a completely random distribution of the molecules as in the isotropic phase, S=0 whereas S=1 in the crystalline state where the constituent molecules are arranged in an orderly repeating pattern that extends over all three spatial dimensions. For a typical liquid crystal sample S is of the order of 0.3 to 0.8, and generally decreases as the temperature is increased.

Refractive index

For a liquid crystal there are two principal refractive indices for a light wave propagating parallel to **n** and perpendicular to **n.** The difference between $\mathbf{n_e}$ the extraordinary refractive index and ordinary refractive index $\mathbf{n_o}$ gives the birefringence of the material. The birefringence is given by

$$\Delta n = n_e - n_o$$

The effect of birefringence is shown below for nematic liquid crystal taken between crossed polarizers(6).

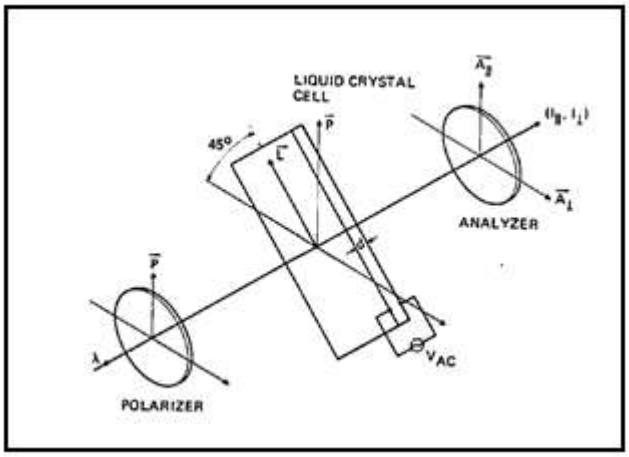

Fig 1.8: Schematic diagram of the arrangement that can be used to observe birefringence of liquid crystals.

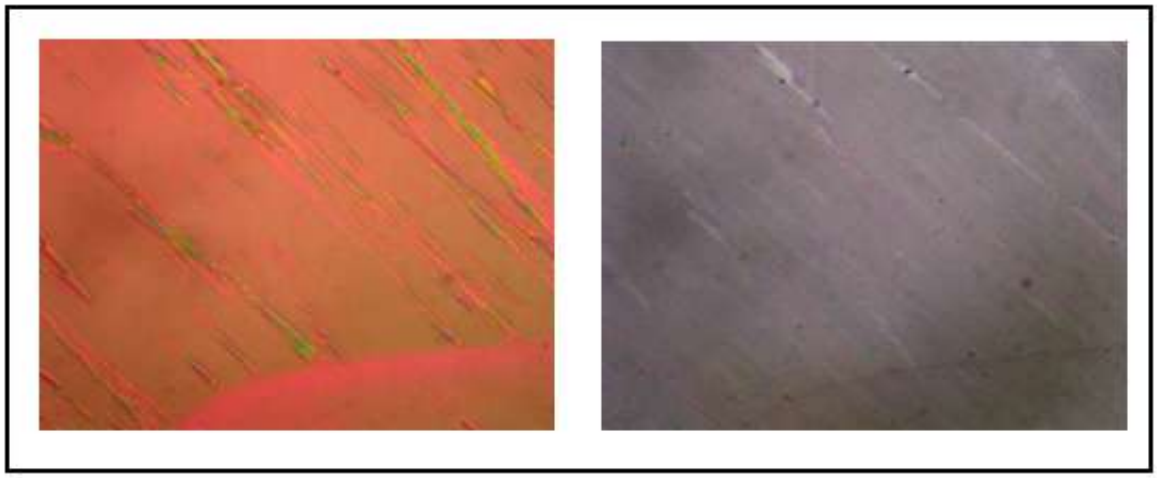

(a) **(b)**

Fig 1.9: Optical textures exhibited in a nematic liquid crystal

Optical textures exhibited in a nematic liquid crystal for different orientations of the polarizers is shown in Fig 1.9

Electrical conductivity

The conductivity of the material mainly depends on temperature and resistance of the material. In liquid crystals the conductivity increases because of residual ionic impurities. The anisotropic conductivity is given by,

$$\Delta\sigma = \sigma_{\parallel} - \sigma_{\perp}$$

where $\sigma_{\parallel}$ and $\sigma_{\perp}$ are the prinicipal components of conductivity parallel and perpendicular to the director.

Dielectric anisotropy

Dielectric constants measure the response of the material to the external field. Liquid crystals are characterized by two dielectric constants $\varepsilon_{\parallel}$ and $\varepsilon_{\perp}$ measured with the applied field along and perpendicular to the director. The dielectric constants measured in a LC have a major

contribution from the orientational polarisation. The dielectric anisotropy of the material is given by

$$\Delta\varepsilon=\varepsilon_{\parallel}-\varepsilon_{\perp}.$$

The sign of $\Delta\varepsilon$ can be positive or negative depending on the permanent dipole moments present in the molecules. If the component of the net dipole moment of the LC molecules is larger along the long axis of the molecule than that along the transverse axis the sign of $\Delta\varepsilon$ will be positive and vice versa.

Elasticity:

There are three different types of elastic deformations in liquid crystals known as the splay, twist, and bend.

The deformation free energy is given by,

$$\frac{K_{11}}{2}(\nabla.\hat{n})^2+\frac{K_{22}}{2}(\hat{n}.\nabla\times\hat{n})^2+\frac{K_{33}}{2}(\hat{n}\times\nabla\times\hat{n})^2=E_d$$

Where K_{11}, K_{22}, K_{33} are the splay, twist and bend elastic constants respectively. $\hat{n}$ is a dimensionless unit vector.

Freédericksz transition

Liquid crystal molecules respond to electric fields. The Freédericksz transition in liquid crystals is produced when a sufficiently strong field is applied to a liquid crystal (LC) in an undistorted state. Below a certain threshold field the director remains undistorted.

The threshold electric field V_{th} is given by

$$V_{th}=\frac{\pi}{d}\sqrt{\frac{K}{\varepsilon_o\Delta\varepsilon}}$$

Where K is the elastic constant and $\Delta\varepsilon$ is the dielectric anisotropy.

1.8 METAL NANOPARTICLES AND THEIR SURFACE EFFECTS

1.8.1. Surface Plasmon Resonance (SPR)

Nanoparticles are typically 1- 100nm in size. They exhibit size dependent properties. Metal nanoparticles are interesting because of their optical properties. Metal nanoparticles are synthesised by several methods in different shapes. Noble metal nanoparticles also support surface plasmons at optical frequencies, known as localized surface plasmons (LSPs). These particles act as dielectric spheres and exhibit strong scattering of the electromagnetic radiation if the size of the sphere is similar to the wavelength of the radiation. If the frequency of the incident wave matches with the plasmon oscillation frequency, a resonance will occur, called the surface plasmon resonance (SPR). The radiation produces the oscillation or perturbation of the electron cloud resulting in a periodic separation of charges within the molecules, which is called as induced dipole moment. These oscillating dipole moments cause the radiation of secondary EM waves. This scattering process was first described theoretically by Mie in 1908 (7).

The surface plasmon resonance frequency of the nanoparticle depends not only on the particle size, but also shape, orientation, diffusion coefficient, surface electrical potential, electron density on the particles and dielectric nature of the surrounding medium.

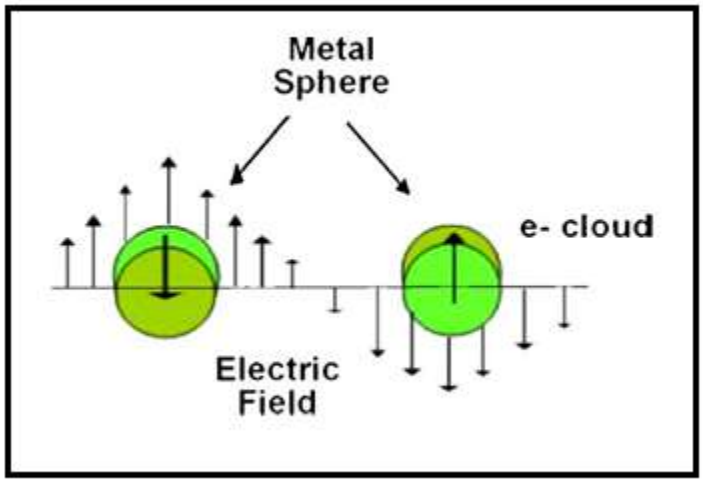

Fig 1.10: Schematic presentation of interaction of spherical nanoparticles with incident Electromagnetic wave.

Mie theory and Discrete Dipole Approximation (DDA) are used to explain the optical effects of the spherical nanoparticles. Mie theory provides an exact description of the interaction of electromagnetic radiation with spherically symmetric particles in a dielectric medium. The theory is exact and accurate in so far as the dielectric functions used to describe the material properly. For metal particles that are small, relative to the electron mean free path, the wavelength-dependent dielectric functions used to calculate the polarizabilities are corrected from their bulk values to account for additional damping of the Plasmon excitations at a nanoparticle surface.

1.9 LITERATURE SURVEY OF RELATED WORK

Synthetic procedures used to prepare gold nanoparticles were surveyed.

Gold nanoparticles can be prepared by various methods. The most frequently used methods of preparation of spherical gold nanoparticles are **Turkevich method** (8) and **Brust method** (9)**.**

1.9.1 Turkevich method

In this method gold nanoparticles are produced by chemical reduction. This method was pioneered by Turkevich and Frens(8). 2ml of hot chloroauric acid was added to 5ml of sodium citrate solution. The colloidal gold forms because the citrate ions act as both a reducing agent, and a capping agent. This solution is heated upto 100^0C. After a defined time, the liquid is extracted and cooled to room temperature. The reduction is achieved by UV irradiation. After exposure 1ml of Ascorbic acid is added. The solution colour is changed from light to dark red colour. The concentration of the sodium citrate changes the size of the nanoparticles. Gold particles can be produced in a wide range of sizes from 9 to 120 nm by this method.

1.9.2 Brust method

In this method gold nanoparticles are produced from organic liquids. It involves the reaction of chloroauric acid solution with tetraoctylammonium bromide (TOAB) which is both the phase transfer and the stabilizing agent. Solution in toluene and sodium borohydride acts as an anti-coagulant and a reducing agent, respectively. This method give particle sizes of around 5–6 nm. It is important to note that TOAB does not bind to the gold nanoparticles particularly strongly, so the particles will aggregate gradually (9). To prevent this, one can add a stronger binding agent,

like a thiol (alkanethiols), which will bind with gold covalently producing a near-permanent solution. Alkanethiols protected gold nanoparticles can be precipitated and then redissolved. Some of the phase transfer agent may remain bound to the particle and after purification may give spherical gold nanoparticles.

Gold nanorods are usually prepared by the following procedure.

1.9.3 Seed mediated method for gold nanorods synthesis

Gold nanorods have been prepared by seed-mediated growth approach in the presence of CTAB surfactant according to the procedure proposed by N.R. Jana (10). It is a two step process, first step is seed preparation process, next is growth process. In the seed process, the seeds were synthesized typically as follows the 20mL aqueous solution containing 0.25mM $HAuCl_4$ and 0.25mM trisodium citrate which acts as capping agent were taken, then 0.6mL of ice cold 0.1 M $NaBH_4$ of freshly prepared solution was added with stirring. The solution immediately turned orange-red, indicating the formation of gold nanoparticles. The average particle size measured from transmission electron microscopy was 3.5nm (10, 11).

The second step is the preparation of growth solution. Gold nanorods were synthesized by the three-step seeding protocol as described previously. The solution of 9 mL of 0.25mM of $HAuCl_4$ and 0.1M CTAB is taken in two conical flasks (A,B) and in the third flask 45 mL (flask C) of growth solution containing a mixture of $HAuCl_4$ and CTAB solution is taken. Then 0.1M of 50µl of ascorbic acid was added into the flasks A and B and 250 µl in flask C and the resulting solutions were stirred gently. The orange colour of the gold salt in the CTAB solution disappeared when ascorbic acid was added. This colour change is due to the reduction of Au 3+ to Au+. When 1.0 mL of the seed solution is mixed with sample A (step1) the solution in sample A develops a red colour thus indicating the formation of gold nanoparticles. After 15 s, 1.0 mL of sample A was mixed with sample B (step 2). This leads to a colour change in sample B, indicating the generation of gold nanoparticles which increase in size. The reduction in this case is slower compared to that in step 1. A 5.0 mL portion of sample B was further added to sample C after 30 s (step 3). The colour of this solution slowly changed to purple. In all cases, each flask was gently stirred to homogenize the solutions. The solution in flask C was kept at 25 °C for a period of 16h. The final product which is a gold nanorod has the aspect ratio of 19.4 $\pm$ 1.4. When the concentration of CTAB is changed different higher order aspect ratio nanorods (NR)

are obtained. The nanorods are covered with multiple CTAB layers that were confirmed by spectroscopic studies. The gold nanobipyramids, nanostars are also synthesised by the seed mediated synthesis method.

1.9.4 Composites of Liquid crystal and gold nanoparticles

Composite materials consisting of liquid crystals doped with nanoparticles have indeed attracted much scientific and technological interest mainly because the incorporation of nanomaterials enhances the electro-optical properties of the liquid crystal itself. Some earlier work on such composites was reviewed. Thiol functionalized gold nanoparticles like decanethiol, Mercaptophenol, SOBP (4-Sulfanyl phenyl -4-[4-(octyloxy) phenyl] benzoate Thiol-functionalized gold nanoparticles have been added with the nematic liquid crystal pentyl cyano biphenyl (5CB) (9). Liquid crystal cells were fabricated from two indium tin oxide (ITO)-coated glass slides that were separated by a 50-µm thick, self-adhesive mylar spacer and sealed with epoxy glue. To avoid a nonuniform liquid crystal alignment, both the cell and the composite were heated to a temperature above the nematic-to-isotropic phase transition temperature before injecting the composite into the cell. Formation of the nematic (N) liquid crystal phase was confirmed by observing birefringence between crossed polarizers. They have verified the stability of the gold nanoparticle in the nematic phase. Finally they concluded that there is small increase in the N-I phase transition temperature of 0.4^0C and a decrease in threshold voltage. A shift of ~8 nm of the surface plasmon resonance peak was also observed in the LC-NP composite with respect to the peak obtained when the particles were suspended in methylene chloride. This is because of the change in the dielectric constant of the surrounding medium. This shows that the gold NPs are now distributed in the LC.

The unique geometry of columnar mesophases are formed by disc shaped molecules. These are known as Discotic liquid crystals (DLCs). DLCs incorporating thiol functionalized triphenylene derivatives with the monolayer covered GNPs have been studied. NMR analysis of the product indicates the presence of triphenylene and hexanethiol moieties. Phase transitions were noted using polarizing microscopy. When the amount of GNP was increased the tendency of phase segregation and decrease of the isotropic temperature were noted (12). The conductivity of DLC-GNP composites is significantly higher compared with the pure Discotic compound.

A detailed characterization of smectic liquid crystal –gold nanosphere composites have shown that the optical properties can be tuned by increasing the volume fraction of the GNPs. The observed dependence of the surface plasmon resonance wavelength on volume fraction of GNPs is in agreement with the effective medium theory (13, 14)

As such liquid crystal nanocomposite hybrid systems may be important for many device applications like opto electronic devices and displays. We have taken up a detailed study of such composites and will be extending the above type of studies to other liquid crystals and different shaped nanoparticles.

1.10 PRINCIPLES AND INSTRUMENTATION

1.10.1 Polarizing Microscope

Polarising microscope is used to study the optical texture and liquid crystal phase stability.

If the sample is isotropic, the polarised light is propagated through it with the same velocity irrespective of the impinging direction.

Light from an ordinary light source vibrates in random directions and is called nonpolarized light. In contrast, when light travels within a single plane it is called linearly polarized light. A polarizing plate (polarizing filter) or polarizing prism is often used as the device to change natural light to linearly polarized light. The primary light polarizing device is the polarizer and the secondary device is the analyzer. When the two are orthogonal to each other the arrangement is referred to crossed polarisers. Parallel polarisers is the state in which the analyzer is rotated to make the direction of the transmitting linearly polarized light match with the polarizer, and the amount of light transmittance is maximized.

The polarising microscope consists of a halogen light source, light is reflected upwards by a mirror, passes through a lens, and is linearly polarized by the polarizer, which can often be rotated by $360^{o.}$ The sample stage in this microscope can be rotated and a hot stage can be placed on the stage. The sample is in a plane perpendicular to the direction of light propagation. The transmitted light then passes into the objective. The textures exhibited by the liquid crystal and

liquid crystal nano composites were studied using such a polarizing microscope between crossed polarisers.

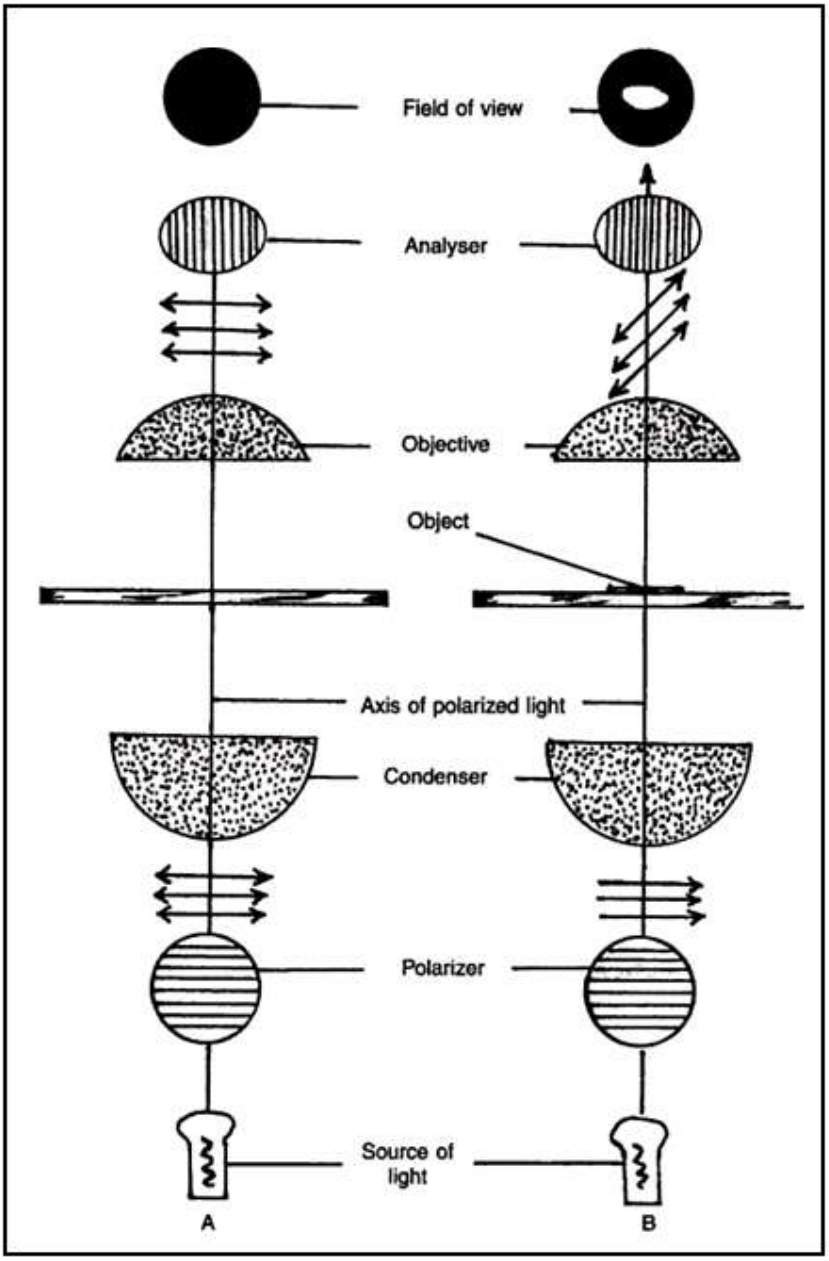

Fig 1.11 : Block diagram of Polarising Microscope(15).

1.10.2 Absorption spectroscopy

A material's absorption spectrum is the fraction of incident radiation absorbed by the material over a range of frequencies. Absorption spectroscopy refers to spectroscopic techniques that measure the absorption of radiation, as a function of frequency or wavelength due to its interaction with a sample. The intensity of the absorption varies as a function of frequency, and this variation is the absorption spectrum. Absorption spectroscopy is performed across the electromagnetic spectrum.

Absorbance spectrometer is used to study the plasmonic absorbance of the metal nanoparticles.

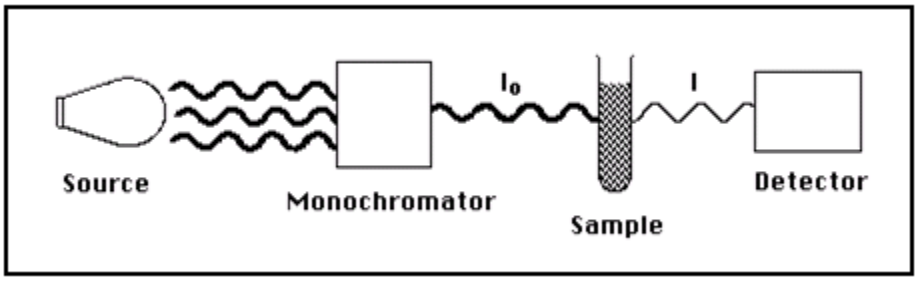

Fig 1.12: Block digaram of Absorbance spectrometer (16).

The Tungsten halogen lamp is used as the source. It produces a continuous spectrum of light in wide range, from near ultraviolet into the near infrared. The grating in the beam path adjusts the wavelength and monochromaticity. The light intensity inside the sample solution is attenuated according to Beer- Lambert law,

$$I_{max}=I_o e^{-\gamma D}$$

Where, D-path length, γ- extinction coefficient

$$\gamma=N\sigma_{ext}$$

Where, N- density, σ_{ext}- extinction cross section

The detector measures the transmitted intensity. By using the T+ E=1, where T- Transmission, E- Extinction.

1.10.3 Transmission Electron Microscopy (TEM)

For imaging the shape and size of the particle we have used the electron microscope because of the high resolution because of the shorter wavelength. So it gives picometer resolution. The conventional transmission electron microscope is a key tool for imaging the internal microstructure of ultrathin specimens. Transmission electron microscopy is one type of high resolution electron microscopy. In Transmission Electron Microscopy (TEM) electron beam is used as source. The beam of electrons is transmitted through an ultra thin specimen, and interacts with the specimen as it passes through. An image is formed from the interaction of the electrons transmitted through the specimen; the image is magnified and focused onto an imaging device, such as a fluorescent screen, on a layer of photographic film or detected by a sensor such as a CCD camera.

The high energy electron beam is emitted by the electron gun made up of tungsten. They are two types of emission- thermionic electron emission and schottky electron emission. The thermionic electron gun is widely used because of high energy electron emission. The electron beam is focused by electrostatic and electromagnetic lenses. The focused electron beam passes through the specimen and the scattered electron gives the structure of the sample. The magnified image is viewed on the detector screen.

The recently developed HRTEM (High Resolution transmission Electron Microscopy) which gives very high resolution image of the sample is a very important tool to analyse the nanomaterials compared to other electron microscopes.

1.10.3.1 Electron diffraction using HRTEM

Electron diffraction is like X-ray diffraction used to study the atomic structure of the sample. The sample material is coated on the copper grid, electron beam passes through it. The electron diffraction pattern gives the sample detail about atomic structure, distance between the two planes. The electron diffraction not only can be used for crystalline material, but can be for amorphous solids, and for studying the geometry of gaseous molecules.

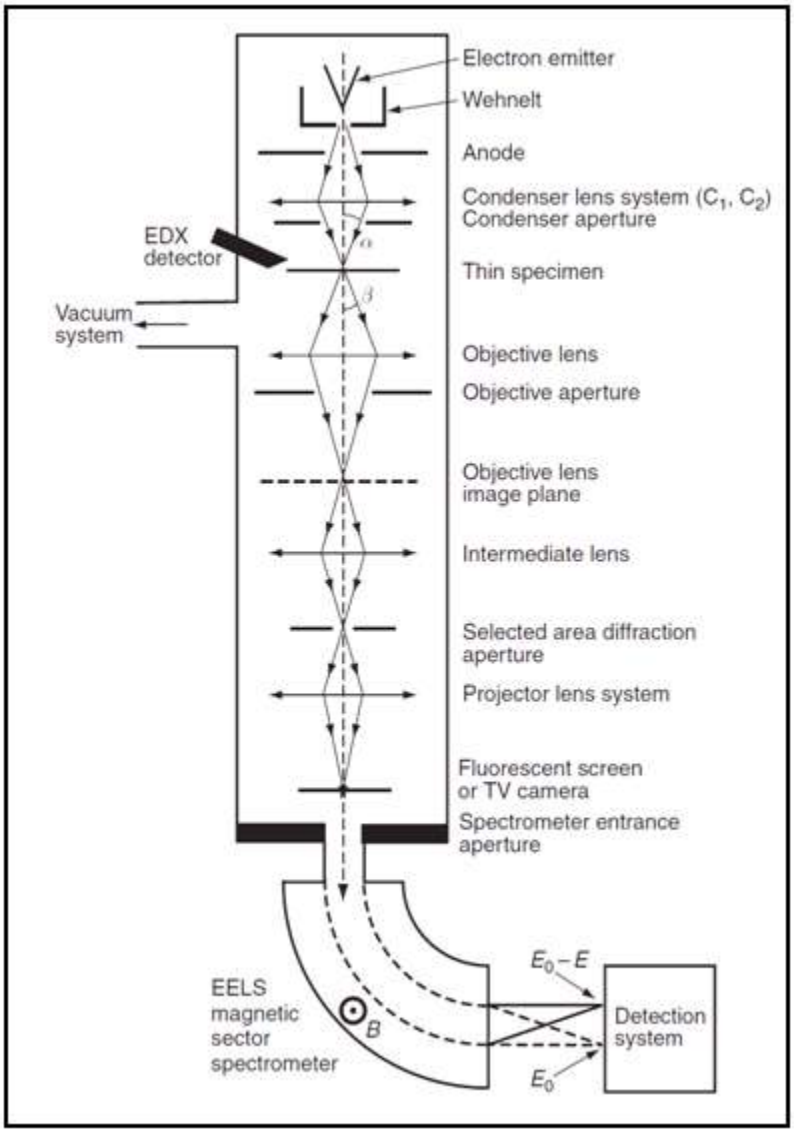

Fig 1.13: Schematic diagram of an analytical transmission electron microscope (17).

1.10.4 Nonlinear optical transmission

Nonlinear optical properties of the sample can be studied using high intense laser light. The transmission of light through a nonlinear medium depends on the characteristics response of the medium to the light. The transmission is affected by the scattering, refraction or absorption by the medium. At sufficiently high input fluence, the probability of simultaneous absorption of more than one photon can be enhanced, Two-photon and multiphoton excitations are examples

for such processes. In addition, intense laser field can lead to population redistribution in complex molecules and the generation of free carriers in solids. Thus the transmittance of the sample will be either enhanced or reduced at high intensities. This change in transmittance of the material, which happens at high input light intensity or fluence, is known as nonlinear transmission measurements. A few major mechanisms control the nonlinear light transmission they are discussed below (18).

Two-Photon Absorption (2PA)

The two photon absorption involves the simultaneous absorption of two photons from an incident field of radiation, resulting in a transition from the ground state to excited state. This process involves different selection rules than those of single-photon absorption.

Excited State Absorption (ESA)

The excited electron often makes a fast transition to one of the intermediate levels in the excited state, before it eventually returns to the ground state. However, the higher lying excited states are usually radiatively coupled to these intermediate levels, and hence, the electron may get excited to these higher states, before completely relaxing to the ground state. This process is known as excited state absorption. The excited state absorption are two types, saturation absorption(SA) and reverse saturation absorption(RSA)

1.10.4.1 Z scan technique for nonlinear optics

The Z scan method provides a sensitive and straight forward method for the determination of the sign and the values of the real and imaginary parts of $\chi^{(3)}$, respectively, proportional to the nonlinear refractive index and the nonlinear absorption coefficient (19).

In the Z scan experiment, a laser beam having Gaussian spatial distribution is first focused by a lens. The beam direction is taken as the Z axis, and the beam focus is taken as Z=0. The sample to be measured is then translated in short steps from negative Z point to positive Z point through the focus. A plot in which the transmission (usually normalized to the linear transmission value) is plotted against Z position (or intensity, since the focusing by the lens ensures different intensities at different Z positions, with the maximum at the focal point, Z=0 is known as Z-scan curve.

There are two variations of the Z-scan arrangement, namely

1. Closed aperture Z scan and

2. Open aperture Z scan.

In the closed aperture technique, an aperture is placed in front of the detector, which has a diameter smaller than that of the beam at that position. It is a method to find out the nonlinear refractive index of a material and hence termed as pure refractive Z-scan. No aperture is used in the open aperture Z-scan. The open aperture Z-scan was used for our study. So some details about the open aperture Z-scan theory is discussed.

Open aperture Z-scan

In this case, no aperture is kept between sample and detector. Therefore, the detector measures all the light transmitted by the sample, excluding scattering losses. Thus, the change in the transmission due to various nonlinear absorption phenomena will be seen in the detector. When the sample is at the focal point, its transmission will be either maximum or minimum, depending on the sign of the dominant nonlinear absorption process. For RSA it will be a minimum, and for saturable absorption it will be a maximum.

In general, an open aperture Z-scan trace will be symmetric with respect to the focus. The normalized transmittance of the medium for a third order optical nonlinearity is given by

$$T = \frac{(1-R)^2 \exp(-\alpha L)}{\sqrt{\pi} q_0} \int_{-\infty}^{\infty} \ln[1 + q_0 \exp(-\tau^2)] d\tau$$

With,

$$L_{eff} = \frac{1-\exp(-\alpha L)}{\alpha}, \quad q_0 = \beta(1-R) I_0 L_{eff}$$

Where I_0 is the peak intensity at the focal point. β denotes the nonlinear absorption coefficient. For a medium that is transparent at the excitation wave length, β will be the two-photon

absorption coefficient. If the medium has some absorption, then β will contain contributions from both SA and RSA.

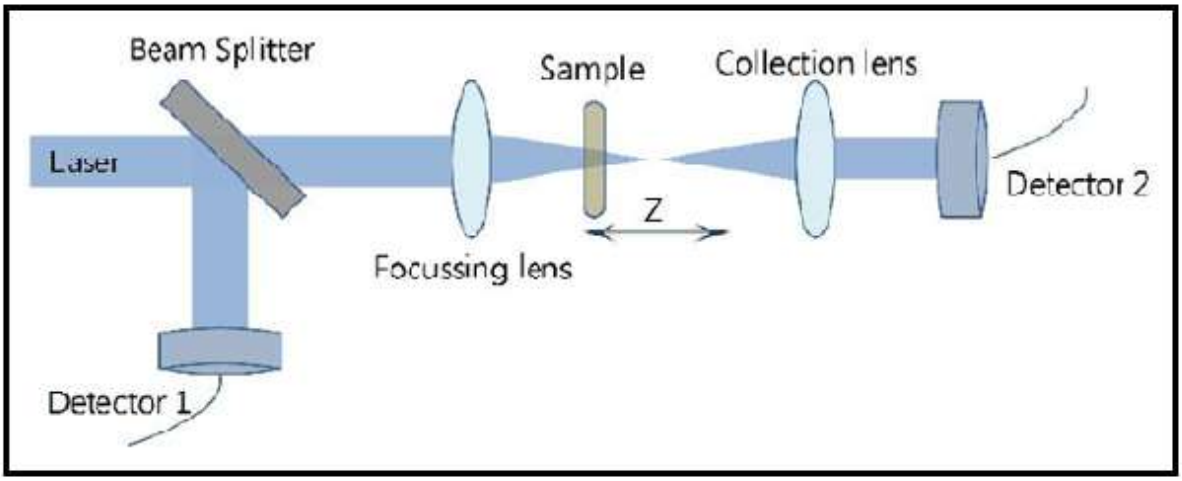

Fig 1.14: Schematic representation of open aperture Z-scan.

A plano-convex lens of 10.5 cm focal length was used to focus the laser beam. The laser is Nd:YAG laser, emitting 5ns pulses. The laser light source emits the wavelength of 532nm of 2.33ev energy. The liquid sample is taken in the 1mm quartz cuvette. The input energy and the transmitted energy by the sample were measured by the two pyroelectric energy probes. The laser pulse to pulse energy fluctuations were generally less than pulse 5% and that was measured by the reference energy probe. The measurements are done in the range between 20000 to 45000 micron distance between the sample and source. There is the successive excitation between the adjacent pulse lasers. The output is monitored by the digital oscilloscope.

1.10.5 Dielectric spectroscopy

Dielectric spectroscopy is based on the phenomena of electrical polarization of the material. There are a number of different dielectric polarization mechanisms operating at the molecular or microscopic level. Each polarization mechanism, either a relaxation or resonance processes, is centered on its particular characteristic frequency, which is the reciprocal of the characteristic time of the process and therefore separable in frequency. The most common mechanisms can be divided into three main categories

- Atomic polarization
- Electronic polarization
- Orientational polarization

At the highest frequencies, the electric field will cause a slight displacement of the electrons of any atom with respect to the positive nucleus, electronic polarization, while at lower frequencies, atomic polarization is due to the distortion of the arrangement of atomic nuclei in a molecule or lattice.

Orientational polarization occurs when particular molecular groups exhibiting a permanent dipole moment, initially orientated randomly in space, tend to be aligned by the applied field to give a net polarization in that direction. The rate of dipolar orientation is highly dependent on inter- and intra-molecular interaction.

Dielectric spectroscopy is also called impedance spectroscopy. The two dielectric constants $\varepsilon_{\parallel}$ and $\varepsilon_{\perp}$ are measured based on a technique similar to the parallel plate capacitor. The Novocontrol Alpha A High performance frequency Analyser is used for these measurements. The liquid crystal sample is taken in appropriate geometry by aligning the director either parallel or perpendicular to the applied field. The capacitance of the confining cell is measured with and without the sample and the values of $\varepsilon_{\parallel}$ and $\varepsilon_{\perp}$ can be extracted from the measured capacitances.

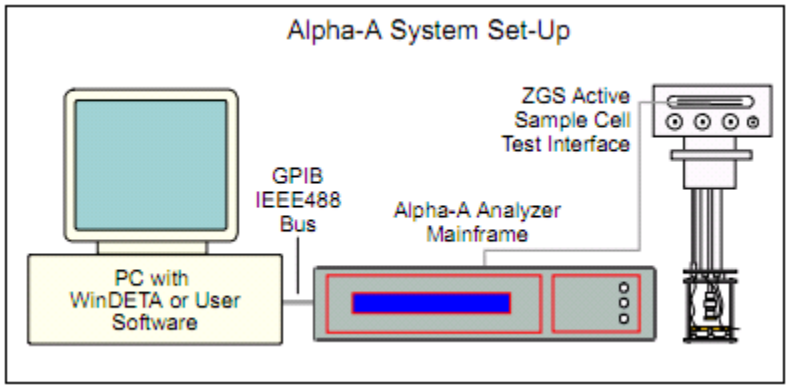

Fig 1.15: Block diagram of Novocontrol Alpha A High performance Frequency Analyser.

1.10.6 Alignments of liquid crystals and Cell preparation

Aligned monodomain samples can be prepared between two substrates with proper treatment of their surfaces. The preparation of cell is discussed below.

1.10.6.1 Cell Preparation

Indium Tin Oxide(ITO) coated glass plate of 1mm thickness. Length of 1.5cm and width of 1cm.

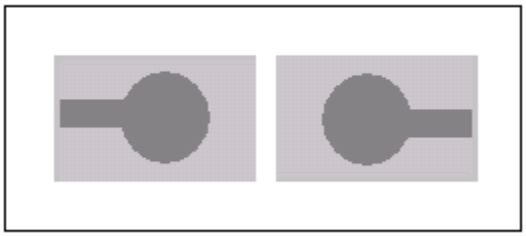

Using wet mask etching 8mm circular pattern is created on the ITO plate.

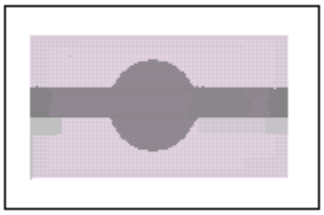

The two plates are overlapped with conducting sides of the etched glass plates facing each other and fixed together with epoxy glue.

Fig 1.16: Schematic diagram of Cell Preparation.

The sample is taken in a cell prepared between two parallel conducting glass plates coated with indium tin oxide (ITO). The width is 1cm and the length is 1.5cm. The plates are patterned to have a circular conducting region with 8mm diameter as the active area. The gap between the two glass plates is a few microns thick. Usually in our experiments ~ 8-12micron thick cells are used.

1.10.6.2 Alignment of Liquid crystals

In order to measure $\varepsilon_{\parallel}$ and $\varepsilon_{\perp}$ it is necessary to align the liquid crystal director either parallel or perpendicular to the glass plates making up the cell. This alignment is achieved by a suitable surface coating on the glass plates.

1. **Homeotropic alignment:** The director **n** is perpendicular to the glass plates. Such a cell can be prepared by coating the glass plates with octadecyl triethoxy silane.

   The ITO coated plate is coated with octadecyl triethoxy silane (ODSE) and it is cured for one hour at 150^0C. ODSE is a long chain molecule which is amphiphilic in nature having a polar group and an aliphatic chain. The polar end group is attracted to the surface of the glass plate and the long aliphatic chain interacts with the alkyl chain of the liquid crystal molecules thus giving rise to perpendicular orientation of the director with respect to the glass plate.

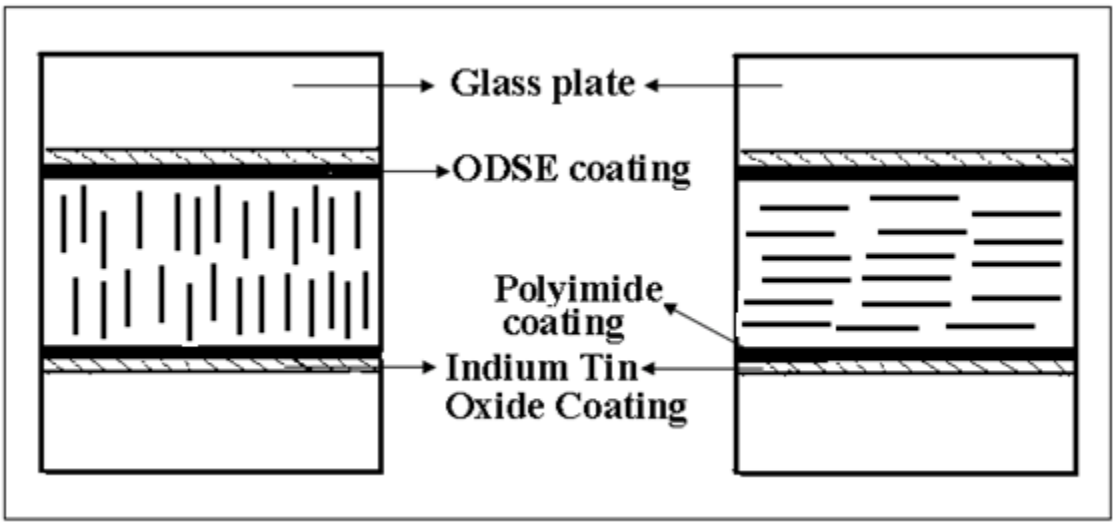

Fig 1.17: Alignment of liquid crystals due to the coating.

2. Homogenous or planar alignment:

The ITO plate is coated with polymide and cured at 280^0c for an hour. Then the plate is rubbed unidirectionally using a soft tissue paper. The cell is prepared such that the rubbing directions of both the plates are parallel to each other. They are then attached by epoxy glue. The cell is cured for one hour at 150^0C, and gives a planar alignment.

1.10.7 Cell thickness measurement

The thickness of the empty cell is measured using fibre optic spectrometer and using ocean optics software controlled by computer. The light reflected normally from the two surfaces of the empty sample cell is captured by the reflection probe made of optic fibres. It is connected to the spectrometer. A spectrum with maxima and minima is seen due to the constructive and destructive interference of light reflected from the two surfaces of the cell enclosing the air gap. The thickness is calculated using the expression

$$d = \frac{\lambda_m \times \lambda_n}{\lambda_m - \lambda_n} \times \frac{n-m}{2}$$

Where $\lambda_m \; and \; \lambda_n$ are the wavelengths corresponding to the m^{th} and n^{th} fringes respectively.

CHAPTER-II

EXPERIMENTAL TECHNIQUES

2.1 SYNTHESIS OF GOLD NANOPARTICLES

The Gold nanoparticles were synthesised by chemical methods. Some gold nanoparticles have been synthesised by two step process. The synthesis of different shapes of gold multi branched nanoparticles was carried out by varying the CTAB concentration and seed solution. The seed mediated synthesis process was used for the synthesis of gold nanoparticles. The list of materials used is given below.

MATERIALS USED	BATCH NO.	MOLECULAR WEIGHT (g/mol)	USAGE
Gold (III) chloride trihydrate	520918	393.83	Source material
Sliver nitrate ($AgNO_3$)	204390	169.87	Shape controller
L-Ascorbic Acid	A5960	176.12	Weak reducing agent
Hexadecyl Trimethyl AmmoniumBromide(CTAB)	H6269	364.45	Phase reducing agent
Sodium citrate	S1804	294.09	Phase reducing agent
Sodium Borohydride	452882	37.8	Nucleating agent

Table 2.1: List of Chemicals used for synthesis.

2.1.1 Synthesis of Gold Nano Pentagons(GNP) of 18.35nm size (sample 1)

The gold nanopentagons had five edges and their shape and size depend on different factors. The particles were synthesised by seed mediated method. The seed solution was prepared and aged for 2 to 5 hours and used for the particle synthesis. The size of the particle depends on the concentration of seed solution, concentration of the CTAB and silver nitrate (20).

Seed solution

The gold nanoparticles seed solution was prepared by adding the following agents i.e. a combination of 0.250ml of 10mM $HAuCl_4$ with 7.5ml of 0.1M CTAB. Then freshly prepared $NaBH_4$ (sodium borohydride) solution of 0.600ml of 0.01M solution was added. $NaBH_4$ is used as a strong nucleating agent. The solution becomes light pink immediately. A minimum time of 2- 3 hours of reaction time is taken after which the seed solution is used. The gold seed solution gave the absorption peak at 533.54nm. The absorption spectra of this sample is shown below.

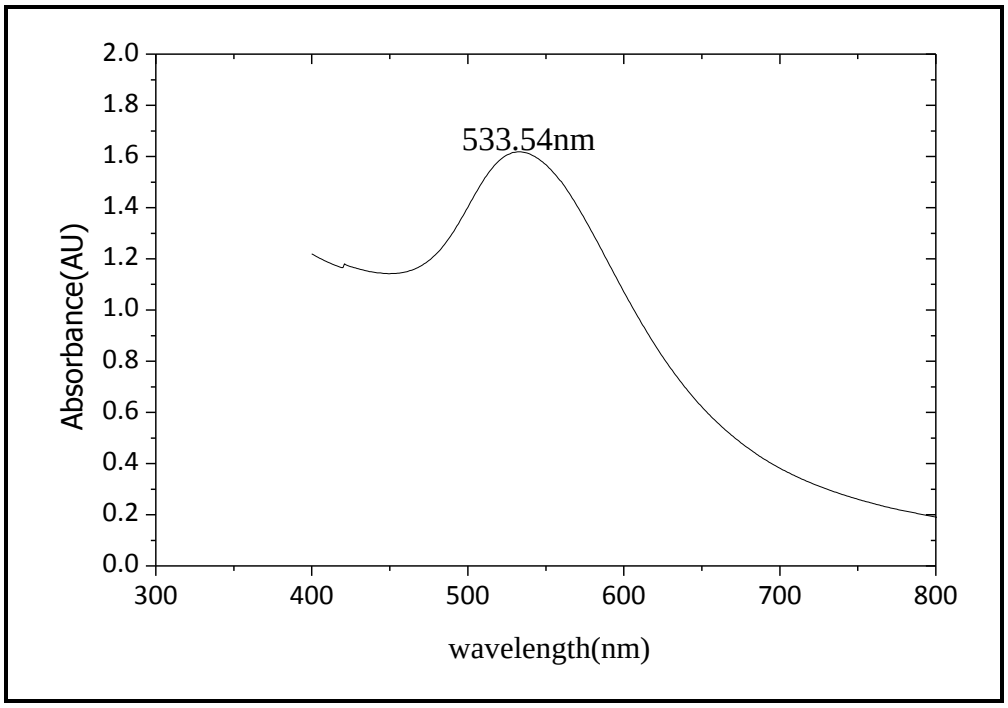

Fig 2.1: Absorbance spectra of seed solution(sample 1).

Growth solution

This is a room temperature synthesis process (27^oC). 4.75mL of 0.1M CTAB (cetyltrimethyl ammonium bromide) is used as the shape templating surfactant. The degree of branching depends on the concentration of the surface capping agent. 0.2 mL of 10mM $HAuCl_4$, and 0.03mL of 10mm $AgNO_3$, silver nitride are used and play an important role in shape control mechanism. The deposition of silver occurs on the crystal faces of gold seed leading to symmetry breaking and multi shape branched gold nanoparticle formation. The solution becomes yellow

brown after addition of 32µl of 100mM of ascorbic acid. It is used as weak reducing agent, that reduces the Au^{3+} into Au^{+} ions. Then 10µl of seed and finally 0.025ml of 0.1M NaOH was added, to improve the reaction. After gentle mixing of the solution for 15 seconds it becomes light purple in colour within two minutes and then becomes dark. If the solution is left overnight in the dark room, the growth solution of gold nanoparticles is obtained. The final absorption spectrum was found to give two peaks probably due to the presence of the few nanorods. Fig 2.2 gives the absorbance spectra of growth solution.

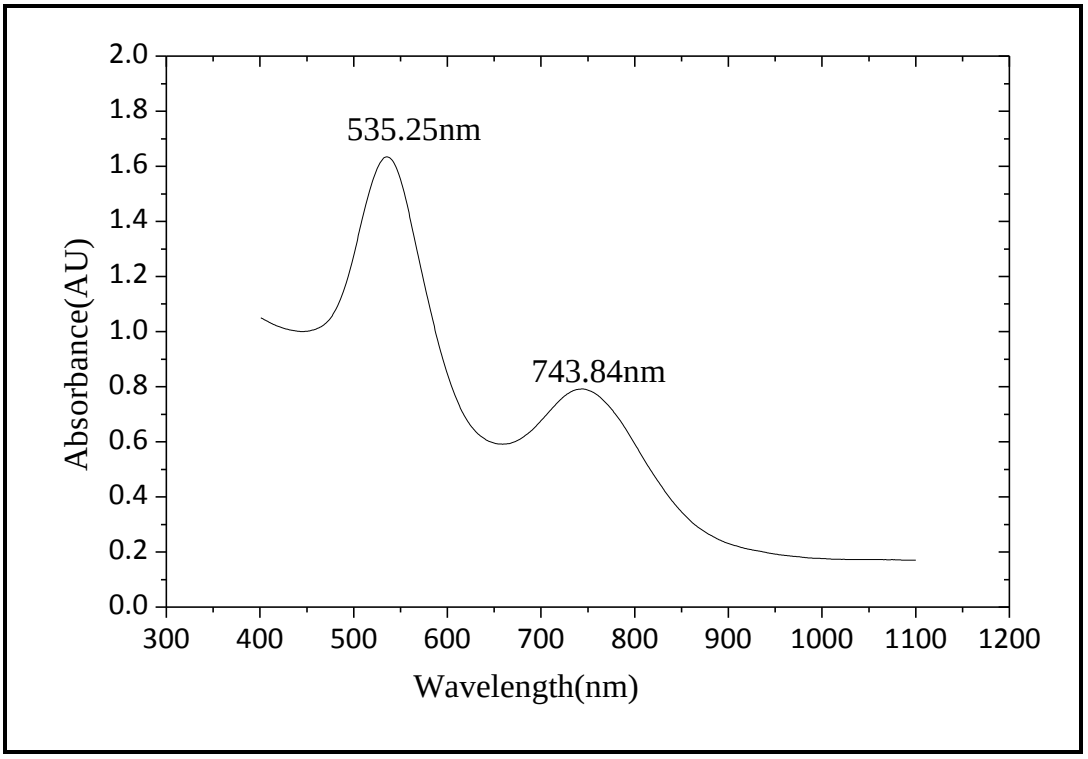

Fig 2.2: Absorbance spectra obtained with gold nanopentagons(sample 1).

TEM Analysis

The shape and size of the nanoparticles was studied by HRTEM analysis. The TEM image of the particles is given in Fig 2.3. The procedure was similar to that is used for synthesizing gold nanostars (REF**). But in our experiment the majority of the particles had a pentagonal shape and were of similar dimension. The average particle size was around 18.35nm. The absorbance due to the particles occurred around 535.25 as a sharp peak.

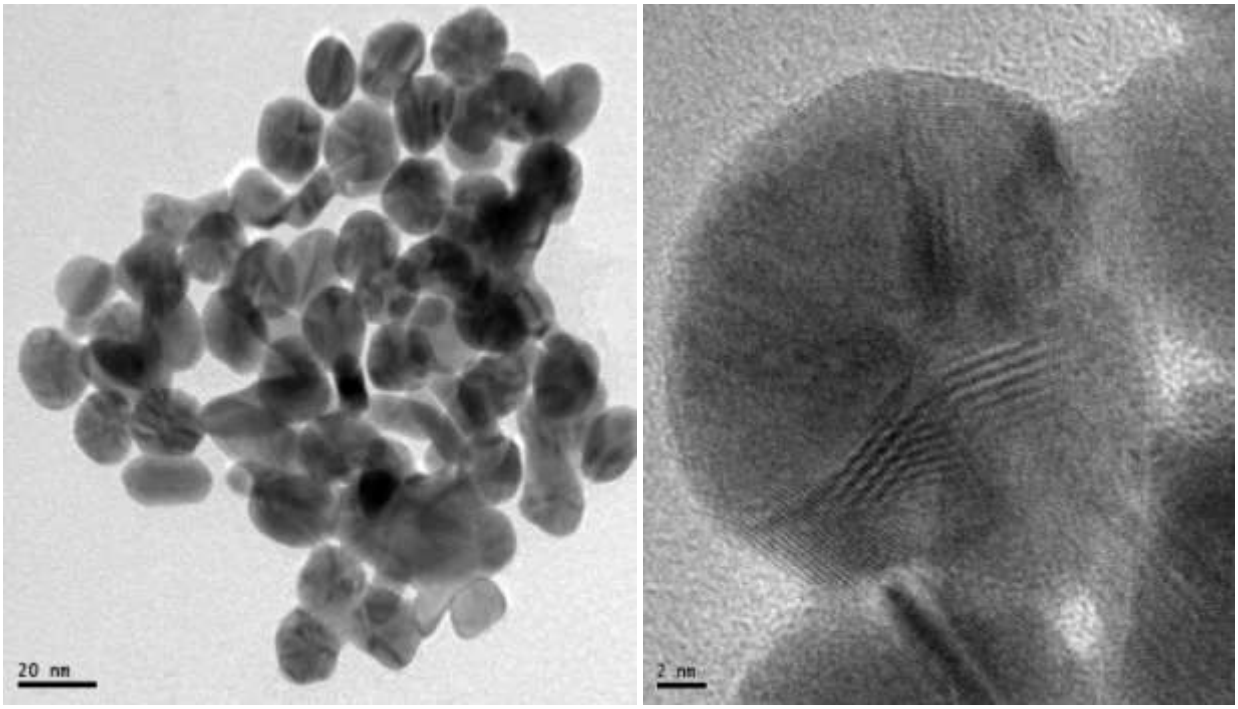

Fig 2.3: TEM images of Gold Nano Pentagons (sample 1).

2.1.2 Gold NanoPentagons of 22.14nm particles (Sample 2)

Seed solution

5ml of CTAB 0.2M is used for shape deformation and added to the 5ml of 0.5mM $HAuCl_4$ solution. The solution is mixed well with ice cold NaBH4. The colour of the solution immediately changed to pale brown. This mixture was stirred for two minutes, then after 2 hours of aging the solution is used for the synthesis of gold nanopentagons(21).

Growth solution

$AgNO_3$(silver nitrate) was used for deprotection. 250µl of 0.004M solution mixed with 0.2M of 5ml solution of CTAB. The solution mixed well and kept at 25^oC for 10minutes. The gold chloride solution of 5ml of 0.001M solution was added to the mixture and the solution becomes

orange in colour. 70µl of 7.88mM Ascorbic Acid is the reducing agent and changes the colour from yellow to colourless, because it reduces the Au 3+ to Au+. 12µl of seed solution was added to the above solution. Then within 1min it changes to coloured solution after continuous stirring of the solution. It is a room temperature reaction and the colour of the solution changed from pink to deep red colour. The solution was left undisturbed overnight. It gave two absorption peaks at 522.92nm and 746.51nm. Fig 2.4 gives the corresponding absorbance spectra.

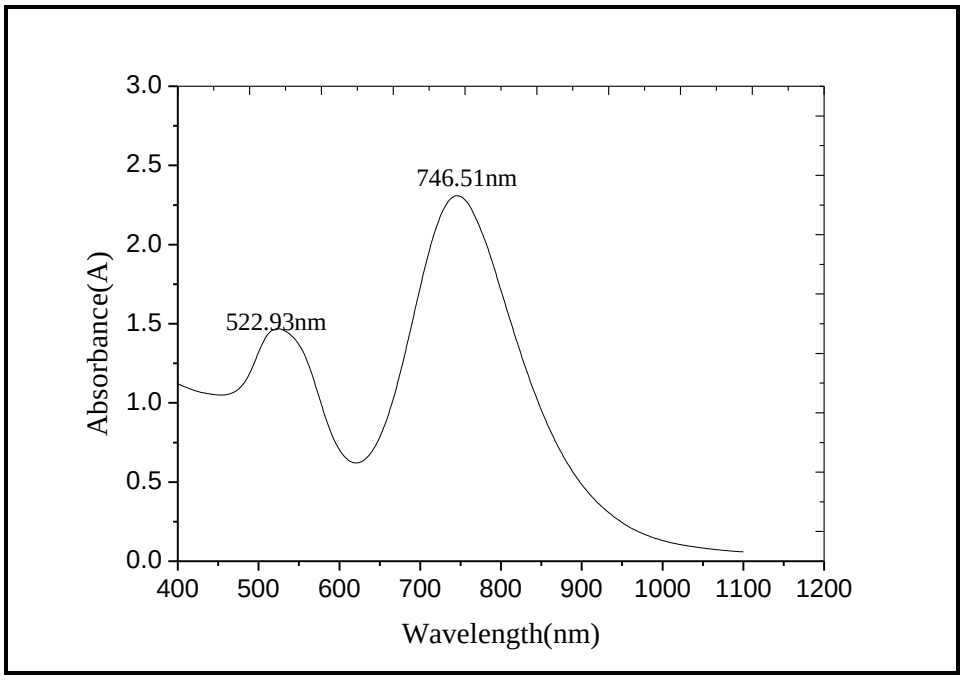

Fig 2.4: Absorbance spectra obtained with gold nanopentagonal(sample2).

TEM images

The size of the gold nanopentagonal particle is 22.14nm, this was conformed by TEM analysis. The TEM image pictures are shown in Fig 2.5.

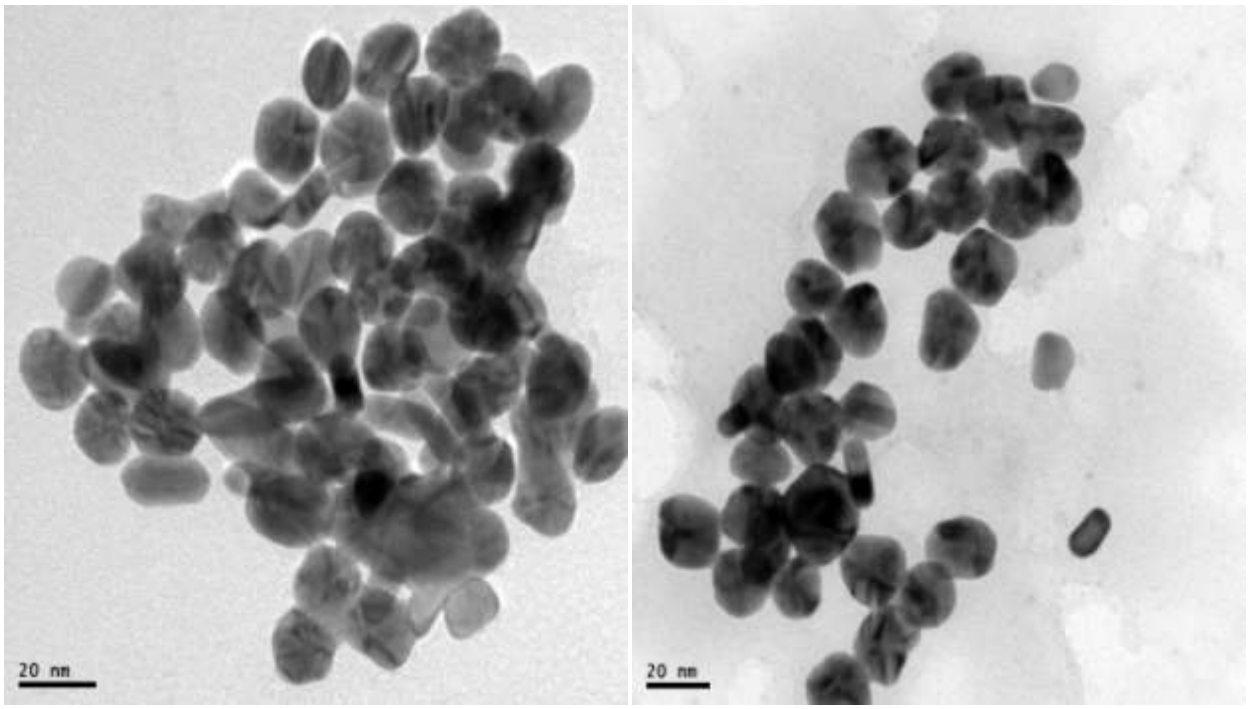

Fig 2.5: TEM images of Gold Nano Pentagons (sample 2).

2.1.3 Nanooctahedral structure

The NanoPentagons are synthesized by seed mediated method, is two step process. But the nanooctahedrons were synthesized by a single step process.

20ml of the solution containing $HAuCl_4$ of 0.125mM and CTAB of 0.01M. CetylTrimethyl Ammonium Bromide (CTAB) is used for the silver and gold nanoparticle synthesis, it acts as phase reducing agent. Ascorbic acid (AA) 0.1M of 100μl was added into the solution. It is an antioxidant and therefore used as reducing agents in the chemical reactions. Finally the sodium hydroxide (NaOH) of 0.1M of 100μl was added to control the PH of the solution. NaOH is more ionic, it contains sodium cations and hydroxide anions (22).

After the addition of NaOH the colour of the solution changes immediately from colourless to light pink colour. Within 10mins the colour changed to pink. The mixture was kept at 50^0C overnight in water bath. The colour changed to purple pink. The particle size depends on the concentration of NaOH. The absorption of the nanoparticle was noted by Perkin Elmer Lambda 38 UV absorption spectrometer. A single peak with absorbance wavelength equal to 544.40nm (after 12 hours) was obtained. Fig 2.6 shows the corresponding absorbance spectra.

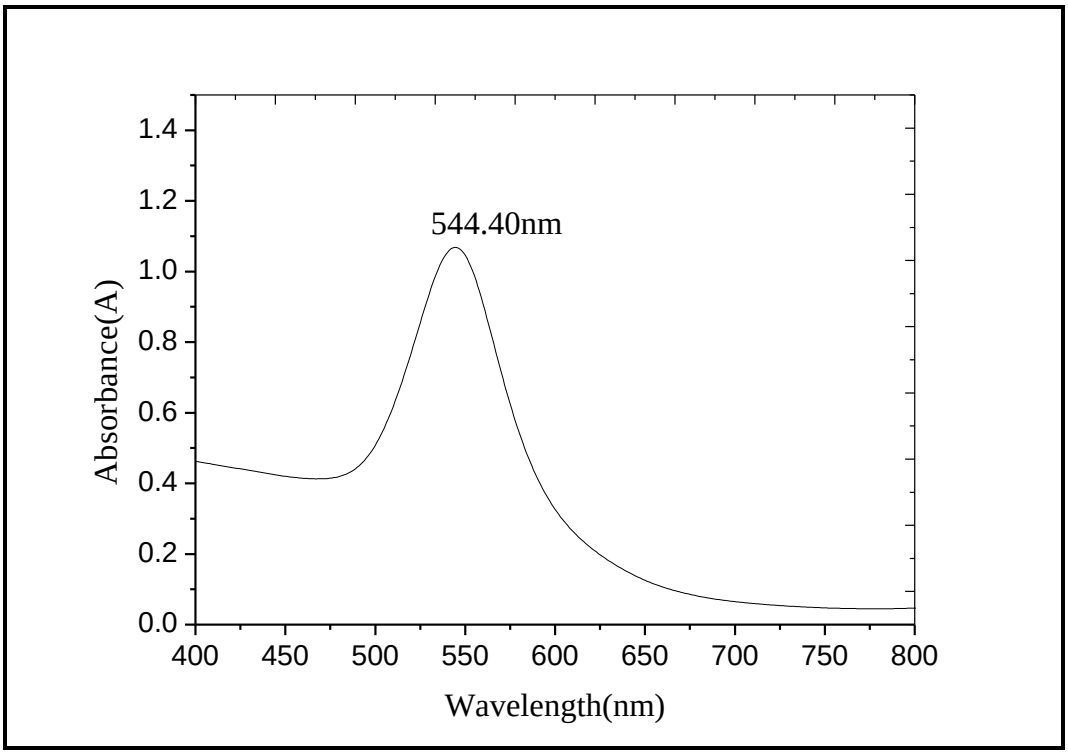

Fig 2.6: Absorbance spectra of Nanooctahedral solution.

2.1.4 Synthesis of Gold Nano Bipyramids

Seed solution

Trisodium citrate was used as reducing agent. The volume of the solution was 9.625ml and contained 0.25ml of 0.01M of gold chloride and 0.25ml of 0.01M trisodium citrate. When 15μl of 0.1M of ice cooled sodium borohydride was added to the solution, the solution becomes orange red in colour. It is used between 2-5hours for the particle synthesis(23).

Growth solution

The shape reducing agent CTAB of 0.1M 7.125ml and 300μl of 0.01M $HAuCl_4$ was added, then 45μl of 0.01M AgNO3 was added. The particle size reduction depends on the solution concentration of silver, ascorbic acid, seed solution. 48μl of 0.1M Ascorbic acid and 12μl of seed solution was added to the mixture. If the concentration of this solution is varied the size and shape of the particles also change. After addition of seed solution the particle will grow in size

and this was confirmed by the colour changes as the starting colour of the solution is violet. The colour first changed to blue and after leaving overnight the solution turns deep blue. The presence of the particles in the solution was confirmed by UV absorbance of the particle. It gave two peaks at 550.11nm and 766.85nm as shown in Fig 2.7.

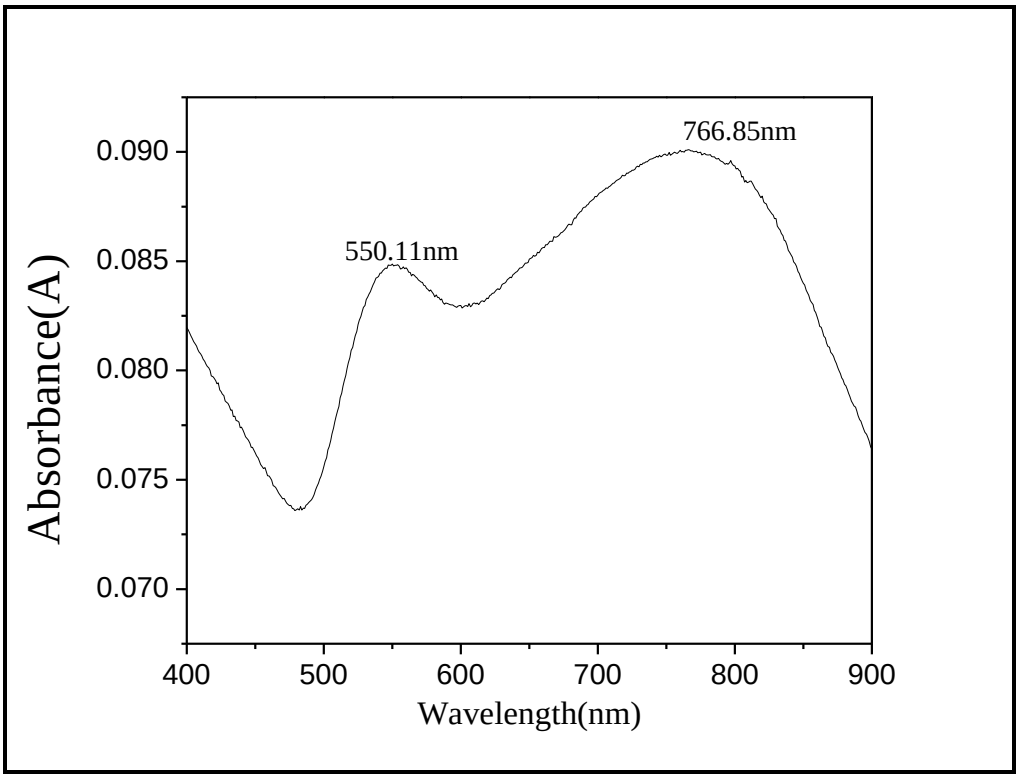

Fig 2.7: Absorbance spectra of Gold Nanobipyramids.

After synthesis of nanoparticles the solution was added to the water and centrifuged for 20minutes at 8000RPM. The particles settled down in the centrifuge tube. Then the procedure was repeated two times to remove the excess CTAB solution. Then the solution was transferred to the organic solution from aqueous solution.

TEM images

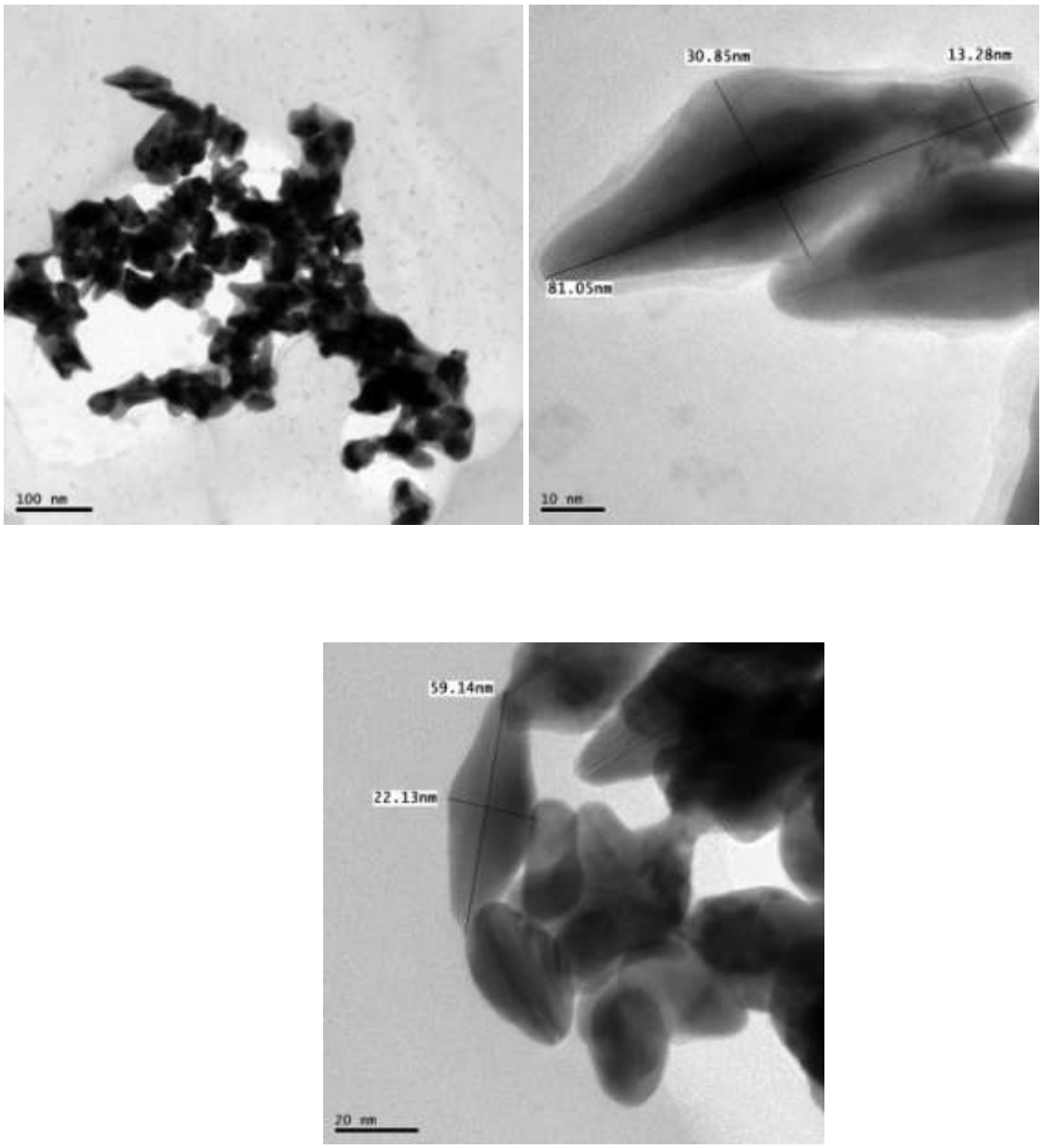

Fig 2.8: TEM image of the Gold Nanobipyramids.

2.2 NONLINEAR TRANSMISSION OF NANOPARTICLES

The nonlinear transmission of nanoparticles was measured using an existing Z-scan experiment setup, (Dr. Reji Philip's lab, Light and Matter Physics, Raman Research Institute, Bangalore, India). The nanoparticles are dissolved in a suitable organic solvent. The sample was then filled in the 1 mm quartz cuvette and loaded as such on a programmable linear translation stage. The

input energy reaching the sample and the energy transmitted by the sample were measured using two pyroelectric energy probes. The laser pulse-to-pulse energy fluctuations were generally less than 5% and were monitored by the reference energy probe. The interval between successive laser pulses was kept sufficiently large to allow complete thermal relaxation of the excited sample between adjacent laser pulses. The energy meter outputs were digitized with the help of a digital storage oscilloscope. The stepper motor was controlled through the parallel port of the PC using appropriate drivers. A detailed schematic experimental setup can be seen in Fig2.9a and the actual laboratory setup is shown in Fig 2.9b.

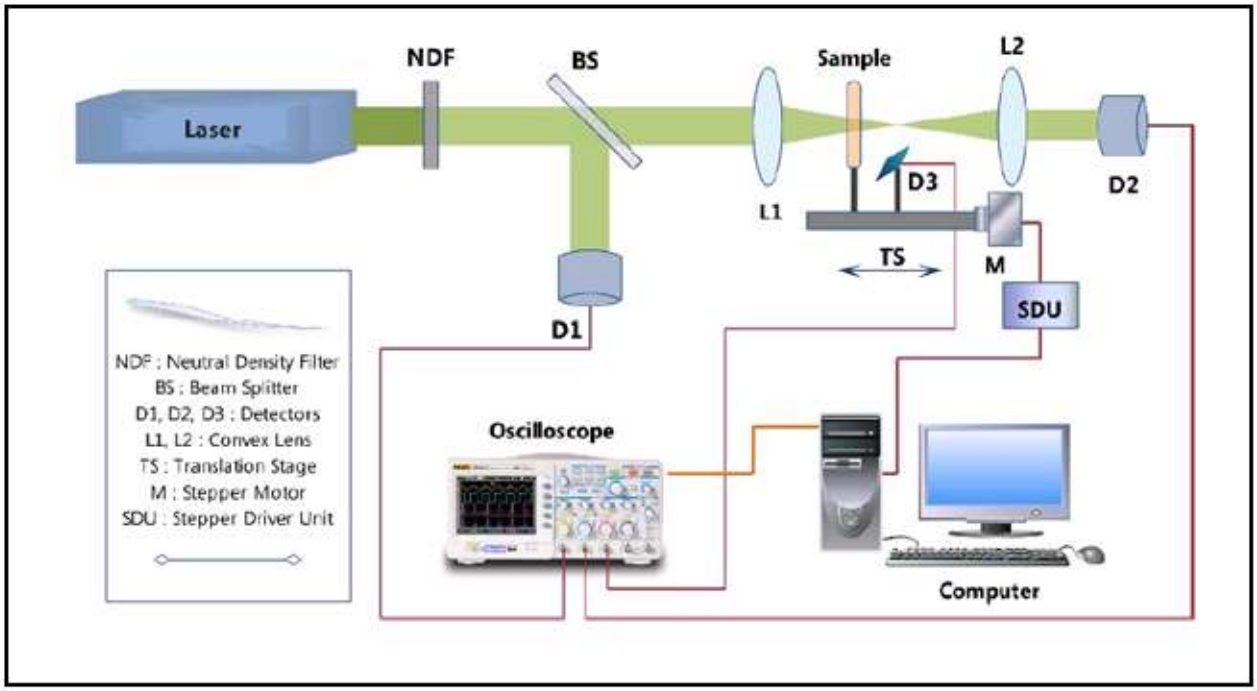

Fig 2.9: Detailed schematic diagram of the Z- scan experimental setup.

2.2.1 The nonlinear transmission measurements

The nonlinear measurment using Z-scan technique were used to measure the nonlinear absoption value of the sample. The sample of gold nano bipyramids particle was dissolved in ethanol solvent. The high intense laser light (wavelength 532nm) was passed through the sample. It has 55% linear transmittance. The sample exhibits two photon absorption. The results are shown in

Fig 2.11. The saturation intensity value is about 3.0 x 10^{13} W/m2. β is the value of two photon absorbance value. Both the saturation graph and fluence curve are shown in Fig 2.11 and 2.12.

Fig 2.10: A photograph of the automated Z-scan setup used for our experiment.

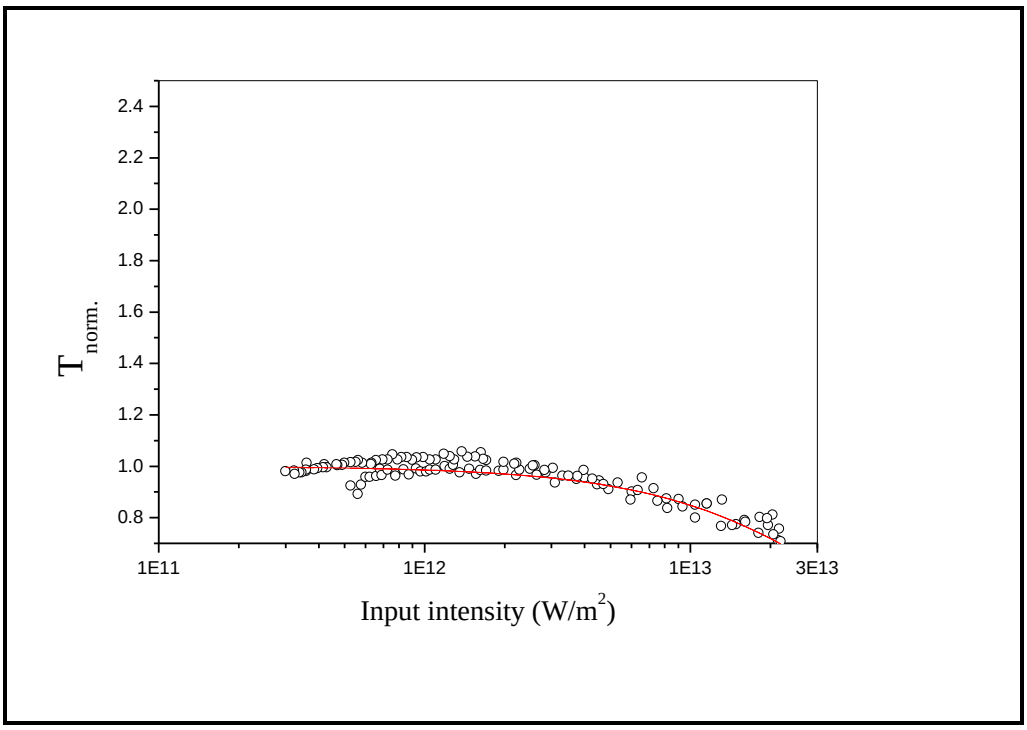

Fig 2.11: Input intensity curve for gold nanobypramids.

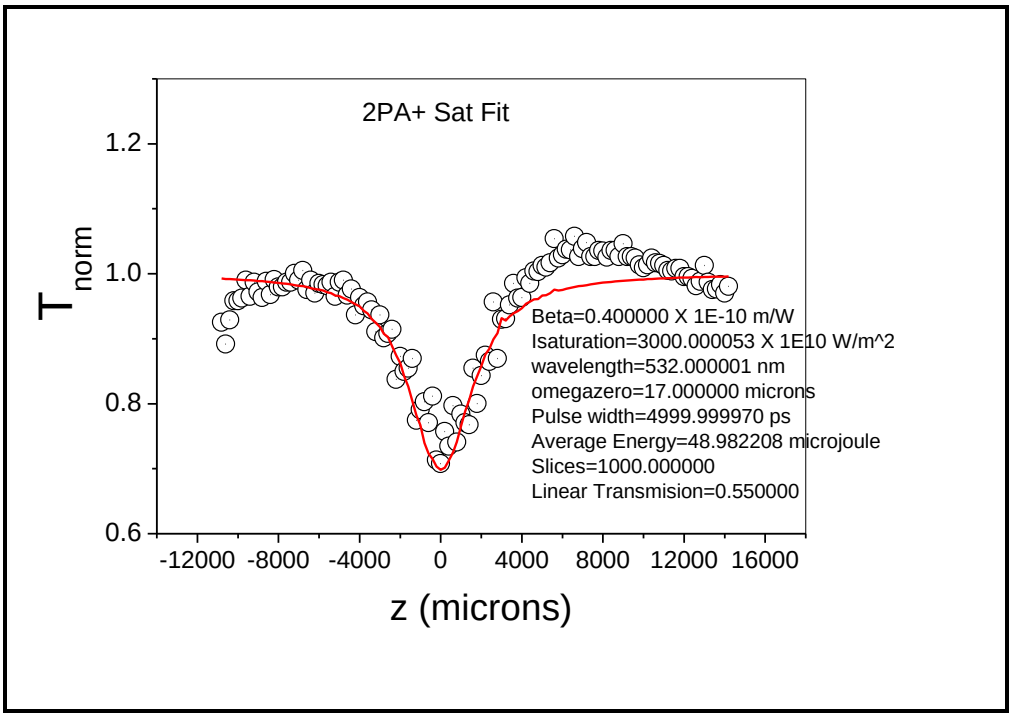

Fig 2.12: Two photon saturation absorption curve of gold nanobypramids.

When the laser is incident on the sample, excitation has taken place from lower energy level to higher energy level because of the high intensity. In this two photon absorption has taken place. The two photon absorbance value of this sample was 0.4×10^{-10}m/W.

2.2.2 Nonlinear optical study of gold nanopentagons (sample 2)

The sample 2 of gold nanopentagons particles were dissolved in the dichloromethane solvent. It showed 70% linear transmittance and it exhibits two photon absorption. The results are depicted in Figure 2.14. The saturation intensity value is about 1.39 x 10^{13} W/m2. β the value of two photon absorbance value for the gold nanopentagons is 309.9999×10^{-12}m/W. Both the saturation graph and fluence curve are shown in Figure 2.13 and 2.14.

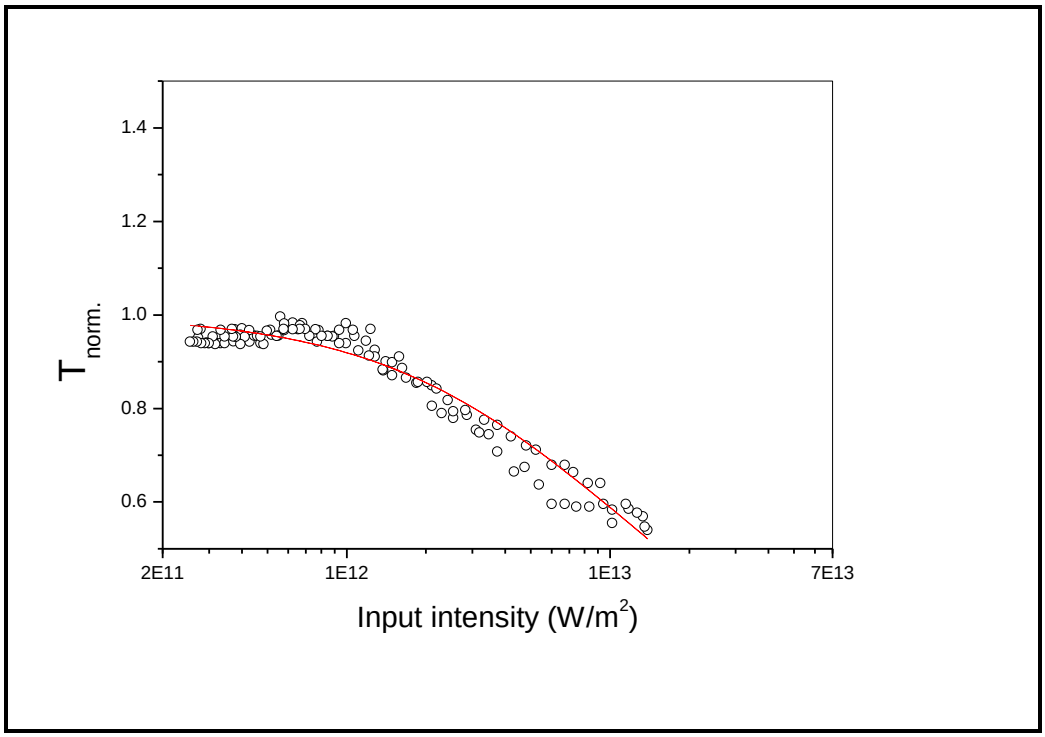

Fig 2.13: Input intensity curve for gold nanopentagons.

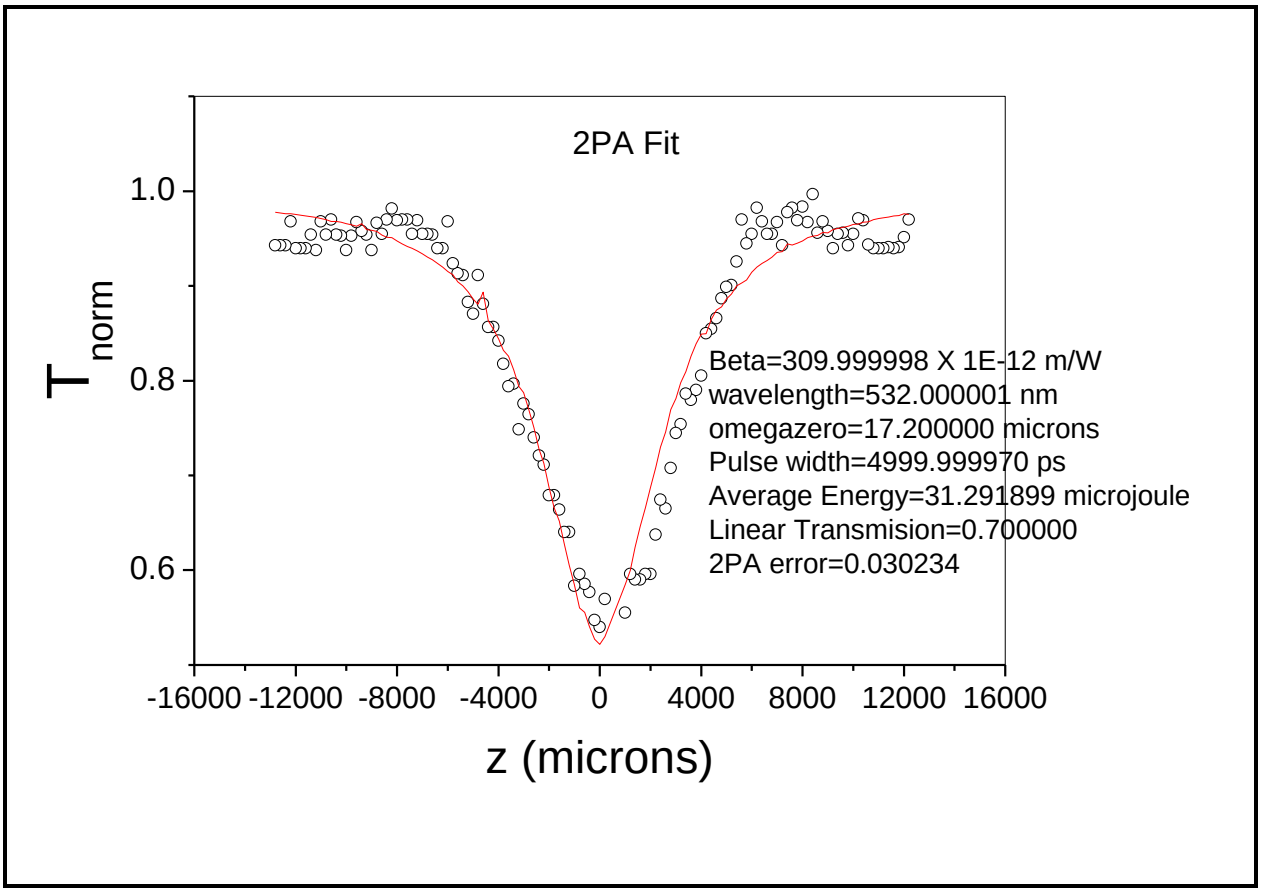

Fig 2.14: Two photon saturation absorption curve for gold nanopentagons.

Sample	β(m/W)	I_s(m/W)
Gold nanobipyramids	0.4E-10	3E13
Gold nanopentagons (sample 2)	309.9999E-12	1.39E13

Table 2.2: Comparison of Z-scan results for Gold nanoparticles.

2.3 DIELECTRIC STUDIES ON PURE E7 AND ITS COMPOSITES WITH GOLD NANOPARTICLES

The room temperature nematic liquid crystal E7 was used for all our studies. E7 is a mixture of four different cyano biphenyl liquid crystals mentioned below.

5CB (4-cyano-4'-Pentyl biphenyl (47 mol %)),

7CB (4-cyano-4'-heptyl biphenyl (25 mol %)),

8OCB (4-cyano-4'-octyloxy biphenyl (18mol %)),

5CT (4-cyano-4'-Pentyl teraphenyl (10mol %)).

In order to see the effect of adding gold nanoparticles into a liquid crystal various physical properties were first measured for E7. The isotropic phase transition temperature of the E7 is 51.1^{o}C. Gold nanoparticles of different shapes were added to the liquid crystal and the properties were again measured. A considerable difference was noted depending on the shape of the particle as discussed below.

The performance and characteristics of display devices critically depend on the physical properties of the liquid crystals. The threshold voltage, elastic constant and the dielectric anisotropy are very important as they measure the distortions of the liquid crystal when an electric field is applied. So we were interested in studying the effect of adding nanoparticles to nematic liquid crystals to see if there is any improvement in the changes of the properties.

2.3.1 DETERMINATION OF THRESHOLD VOLTAGE (V_{th})

2.3.1.1 Determination of threshold voltage (V_{th}) for pure E7

A planar aligned sample was used to measure the threshold voltage using the Freederikz transition technique. Usually 8- 12 micron thick sample cells were used for the analysis. When an electric field is applied to the sample, the molecules start reorienting parallel to the field direction at a specific voltage which corresponds to the threshold voltage. This can be recognized as a change in birefringence. With further increase in voltage the birefringence decreases. Fig 2.15 shows the variation of the threshold voltage with temperature for E7.

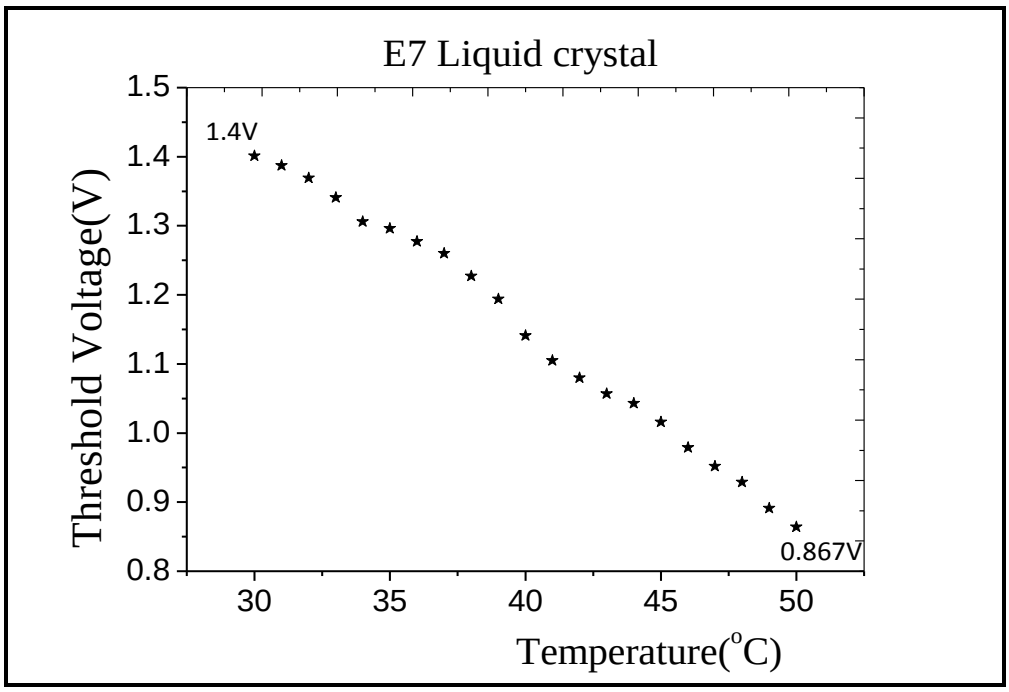

Fig 2.15: Variation of the Threshold voltage with temperature for pure E7.

Fig 2.16: Optical textures exhibited in the nematic phase of pure E7

(a) Planar aligned sample (b) Homeotropically aligned sample.

2.3.1.2 Determination of Threshold Voltage For LC- Gold Nanopentagon composites

The gold nanopentagons with the size of 22.14nm sample were used for the further studies. Two concentrations $C_{0.250}$ and $C_{0.150}$ of gold nanopentagons were mixed in the liquid crystal. The particle solution with gold nanopentagons of solution was added with 5mg of pure E7. The solution was dispersed in dichloromethane solution. These two solutions are mixed well and sonicated for 3- 5 hours. Finally the solvent was evaporated fully, composites were filled in the Planar and Homeotropic cells.

Determination of threshold voltage (V_{th}) for LC- $C_{0.150}$ con. Gold nanopentagons:

($C_{0.150}$= 0.150mg of Gold NanoPentagons + 5mg of E7)

The isotropic phase transition temperature of the sample is 49.2^{o}C. The optical texture of the composite is shown in Fig 2.18. The LC-nanocomposite sample was filled in the Polyimide coated cell for the measurement of the threshold voltage and an AC electric field (1KHz) was applied across the glass plates. Fig 2.17 shows the variation of the threshold voltage with temperature for E7. The threshold voltage of the composite is lower than that of pure E7 because of the nanoparticles.

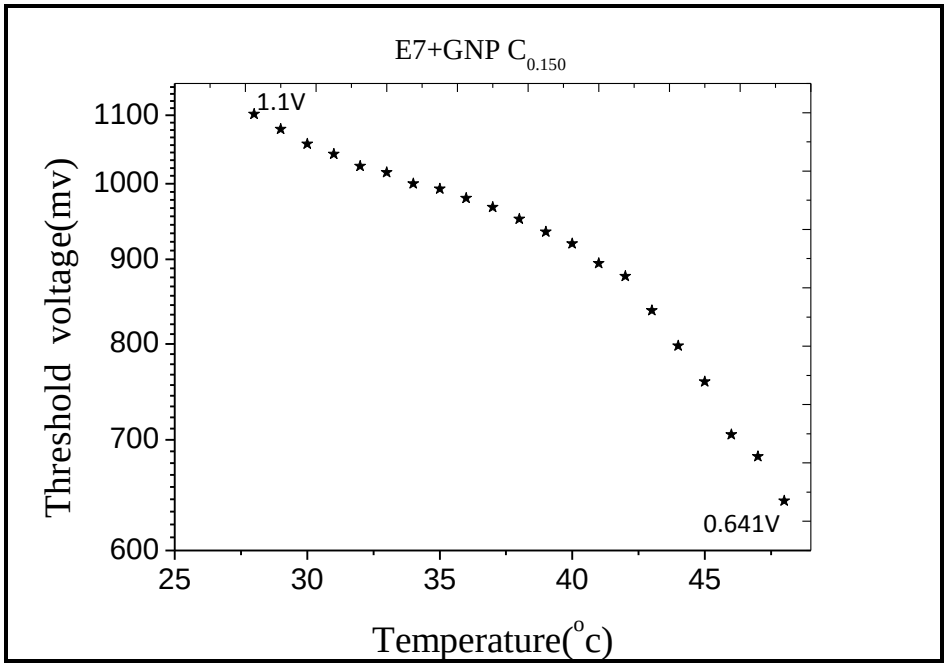

Fig 2.17: Variation of the Threshold voltage with temperature for E7 +GNP$C_{0.150}$.

Here the threshold voltage varied with the concentration of the particles and the temperature. At room temperature the threshold voltage is maximum. The optical textures of the liquid crystal-nanocomposite are shown below. This show that there is no overall change in the liquid crystal phase stability by the addition of the nanoparticles and the optical texture looks similar to that obtained with pure E7.

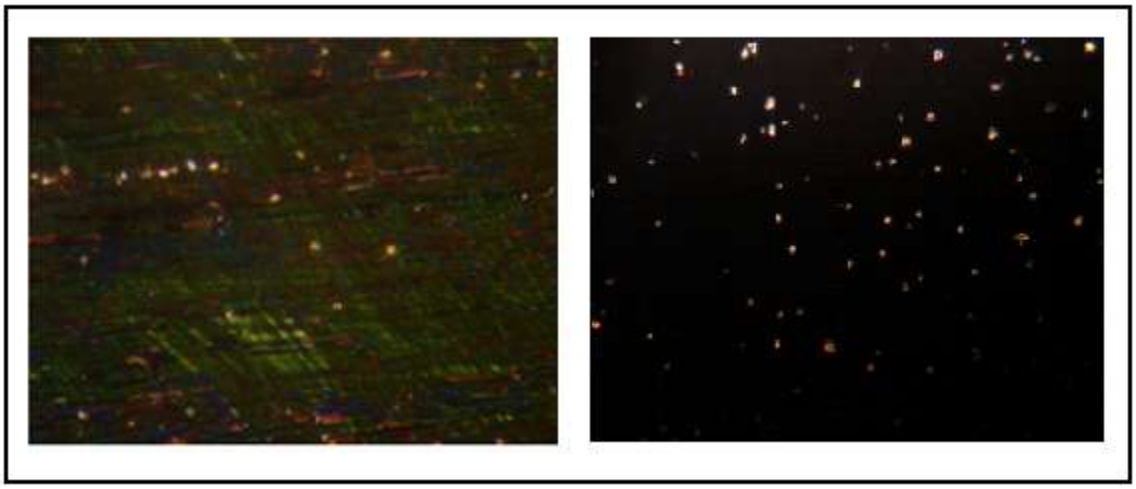

(a) (b)

Fig 2.18: Optical textures exhibited in the nematic phase of LC- Nanocomposite($C_{0.150}$)

(a) Planar aligned sample (b) Homeotropically aligned sample.

Determination of threshold voltage (V_{th}) for E7 - Gold nanopentagons (GNP)$C_{0.250}$ composite

(C_1= 0.250mg of Gold NanoPentagons +5mg of E7)

The particle solution has 1mg of particle per 1ml of dichloromethane. The 0.250ml of solution is transferred to the sample cup. 5mg of the liquid crystal is dissolved in 1ml dichloromethane solution. These two solutions are mixed well and sonicated for 3hours. Finally the solvent was evaporated completely and the composites were filled in the Planar and Homeotropic cells. The isotropic phase transition temperature of the composite is 47.6^{o}C. Compared with the pure sample the isotropic temperature was reduced for the composite because of the presence of the gold nanoparticle. The optical textures are shown in Fig 2.20. The optical texture is shown in

Fig2.16. The optical textures do not show any significant difference with the pure E7 textures. This indicates that the liquid crystalline phase stability is not affected much even when the concentration is increased further.

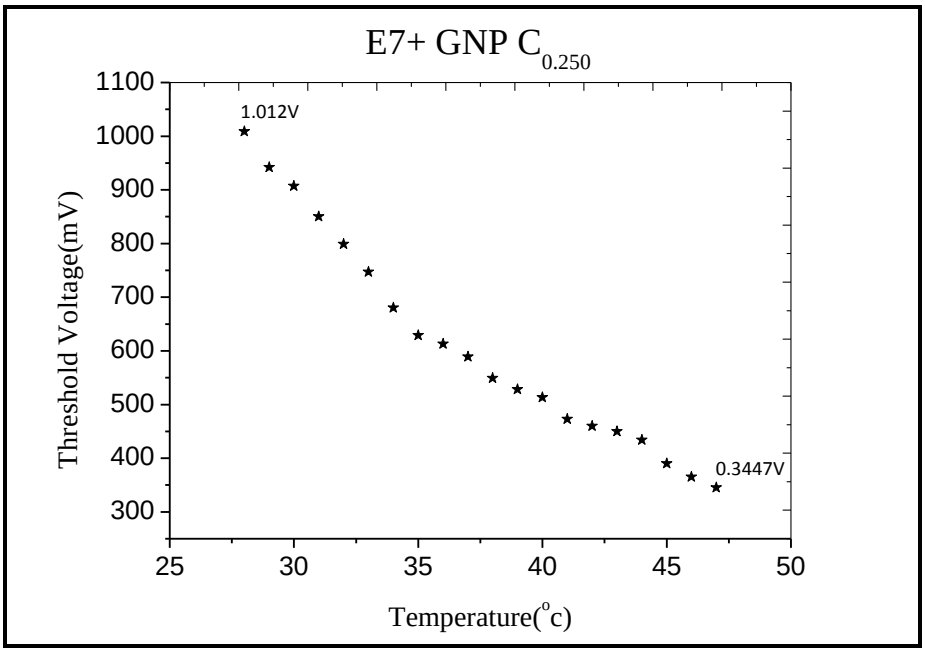

Fig 2.19 :Variation of the Threshold voltage with temperature for E7+ GNP $C_{0.250}$.

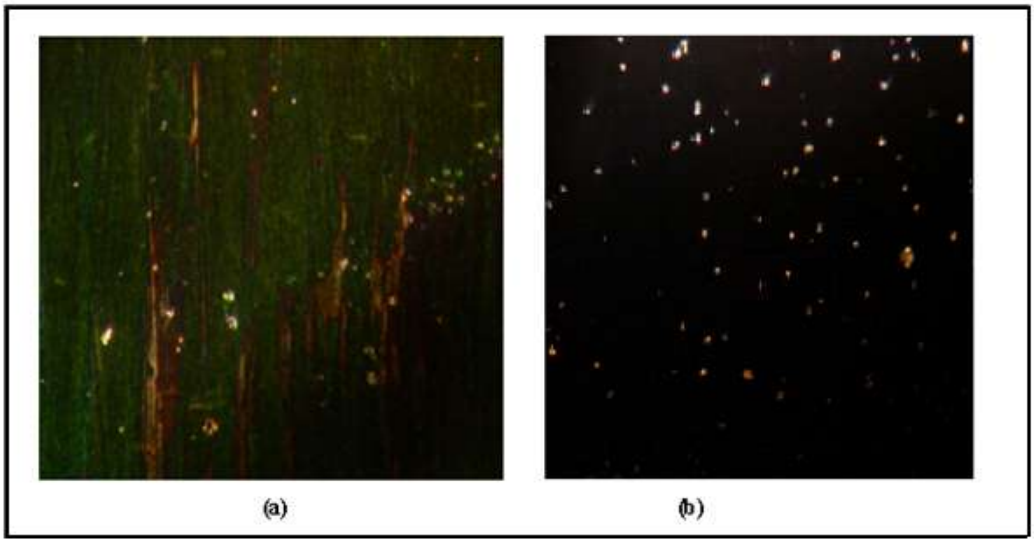

Fig 2.20: Optical textures exhibited in the nematic phase of LC- Nanocomposite($C_{0.250}$)

(a) Planar aligned sample (b) Homeotropically aligned sample.

Gold NanoPentagons of 18.35nm (sample 1) with E7

The gold NanoPentagon particles in ethanol solution of 0.5mg were added with the LC of pure E7 and the sample is filled in the cells. The dielectric studies are done for the sample. The isotropic phase transition temperature of this composite was 49.4^{o}C. The homeotropic and planar aligned sample pictures are given in Fig 2.22.

Determination of threshold voltage (V_{th})

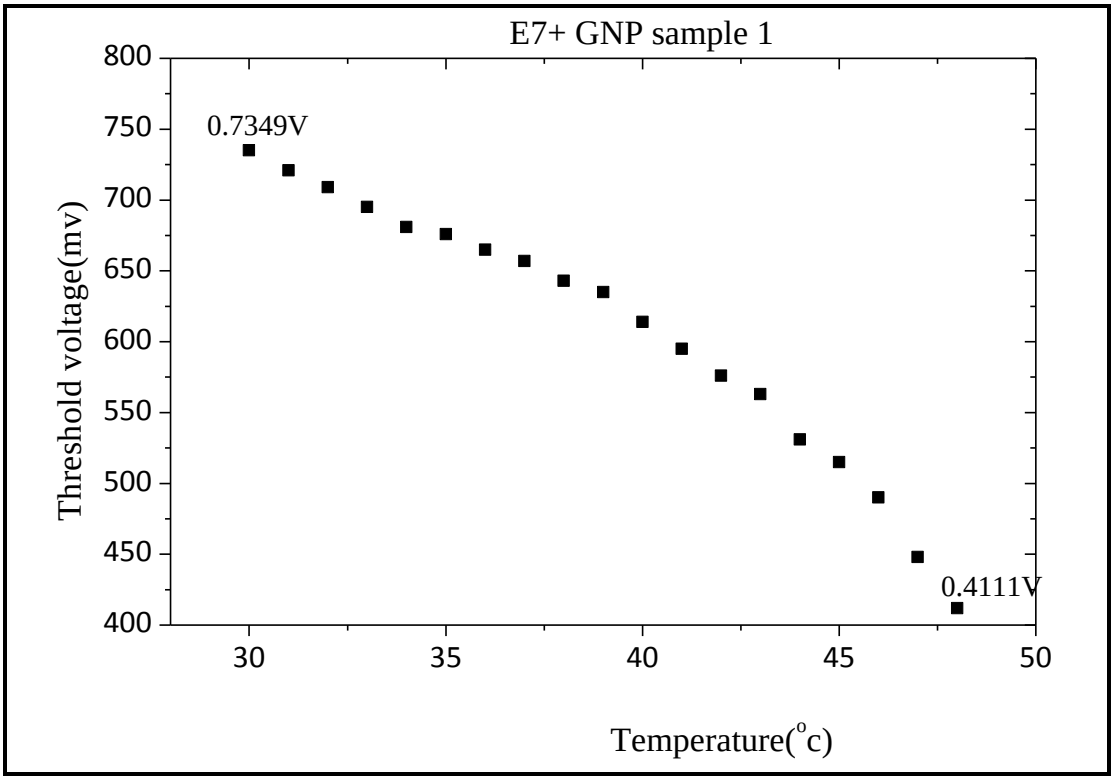

Fig 2.21: Variation of the Threshold voltage with temperature for E7+ GNP(Sample 1).

The frequency was set as 1 KHz, then the temperature was varied from room temperature to isotropic phase transition temperature and the threshold voltage value was noted by observing the change in birefringence under a polarising microscope as described before.

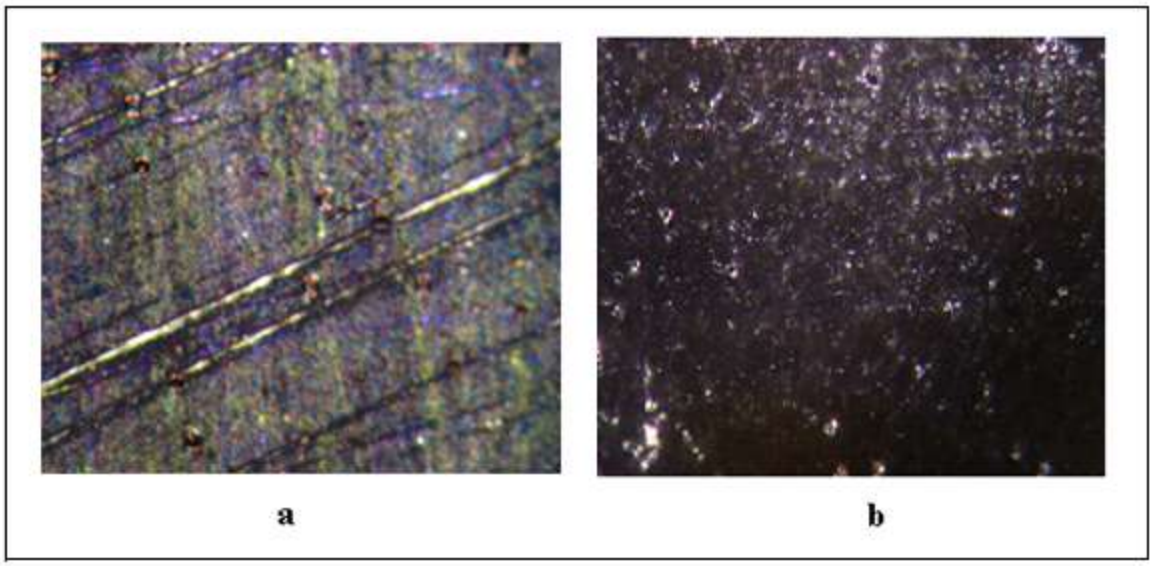

Fig 2.22: Optical textures exhibited in the nematic phase of LC- Nanocomposite (particle size 18.35nm) (a) Planar aligned sample (b) Homeotropically aligned sample.

2.3.2 DIELECTRIC STUDY OF THE LIQUID CRYSTAL AND LIQUID CRYSTAL NANOCOMPOSITES

High dielectric constant materials are used in electronic industry. One method of obtaining such materials is by having composites. We have therefore added high concentration of gold nanopentagons to sample I and sample II in E7 and measured the dielectric constant. The dielectric constants were found to increase ~ roughly twice the value obtained for pure E7. Inspite of adding high concentration nanoparticles the liquid crystalline phase remains stable. The optical texture appeared similar to pure E7 showing that there is no phase segregation. The isotropic- nematic phase transition are clearly shown in dielectric run. This showing that the properties of the nematic phase remain even in composites showing high dielectric constant. When the concentration was increased further the dielectric constant increased significantly.

The thickness of the empty sample cell was measured by Ocean Optics S2000 fiber optic spectrometer and the empty capacitance of the sample cell measured by Novocontrol high performance frequency analyser. After the capacitance measurement the sample is filled in the cell. Properties like conductivity, permittivity, and elastic constant of the sample were studied.

Using the threshold voltage and the dielectric anisotropy the splay elastic constant was calculated using the equation,

$$K_{11} = \frac{\varepsilon_o \, \Delta\varepsilon \, V_{th}}{\pi}$$

Here ε_o permittivity (8.854×10^{-12} F/m), $\Delta\varepsilon$ Dielectric anisotropy, V_{th} thereshold voltage.

The permittivity was measured using both homeotropic and planar cells in order to get $\varepsilon_{\parallel}$ and $\varepsilon_{\perp}$ respectively. For the temperature run the frequency was fixed as constant value, for this analysis 1KHz or 10KHz input frequency was given to the sample by the frequency analyser. The sample was kept in a temperature controller and heated upto the isotropic phase temperature. The measurements were taken in the cooling cycle.

2.3.2.1 Dielectric study for pure E7

Dielectric permittivity for the Pure E7

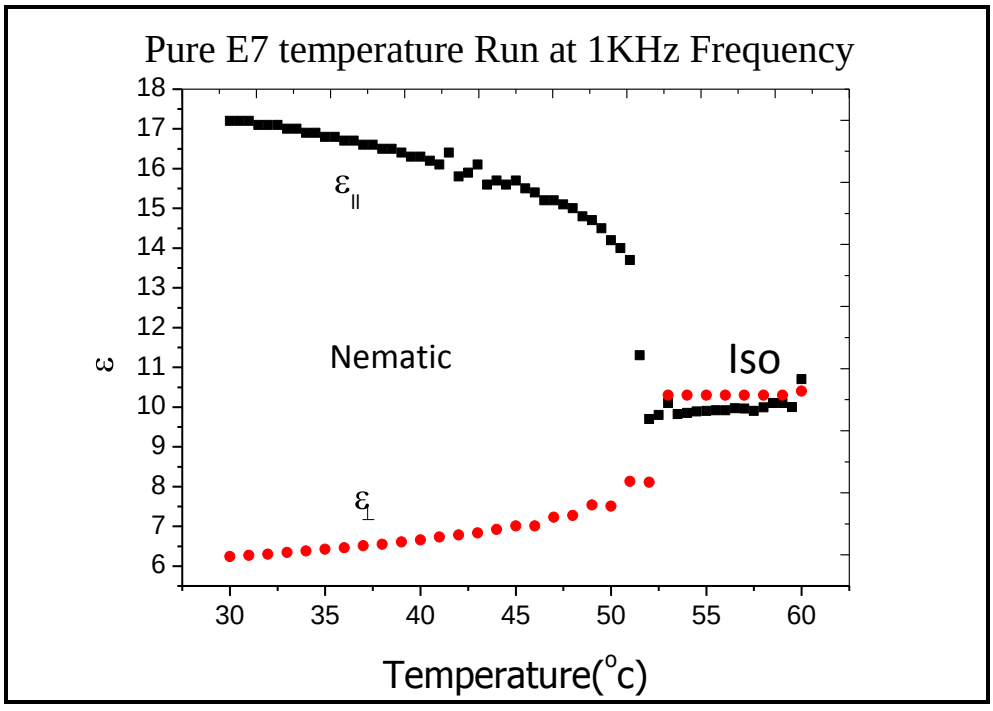

Fig 2.23: Dielectric permittivity for pure E7 at 1KHz

In homeotropically aligned cells permittivity is nearly 17.5 and in the planar cell has permittivity is 6.2 at room temperature. The dielectric anisotropy of the material is given by the equation,

$$\Delta\varepsilon=\varepsilon_{\parallel}-\varepsilon_{\perp}$$

The dielectric anisotropy of the material depends upon the applied voltage, frequency, Temperature etc. The dielectric anisotropy of the material changes with the increase in the frequency. In isotropic phase they have the same permittivity in both the cells. The temperature run was done at 10 KHz frequency also. The input frequency altered the permittivity compared to the previous 1KHz temperature run.

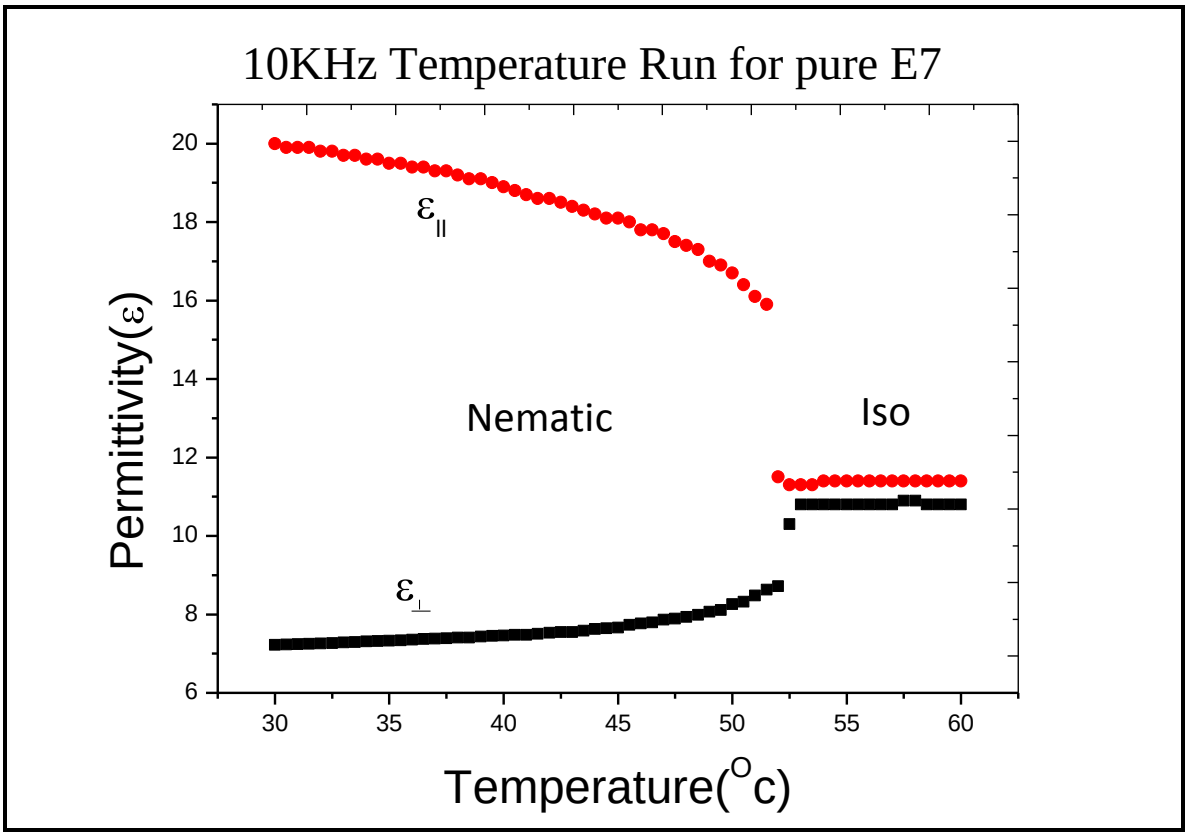

Fig 2.24: Dielectric permittivity for pure E7 at 10KHz

Conductivity Studies for pure E7:

The conductivity (unit is S/m) of the pure E7 sample was measured using the Alpha Novocontrol High performance frequency analyser. The conductivity of the material is increasing when the temperature is increased. For pure liquid crystal the conductivity is of the order of 10^{-9}- 10^{-8} (S/m).

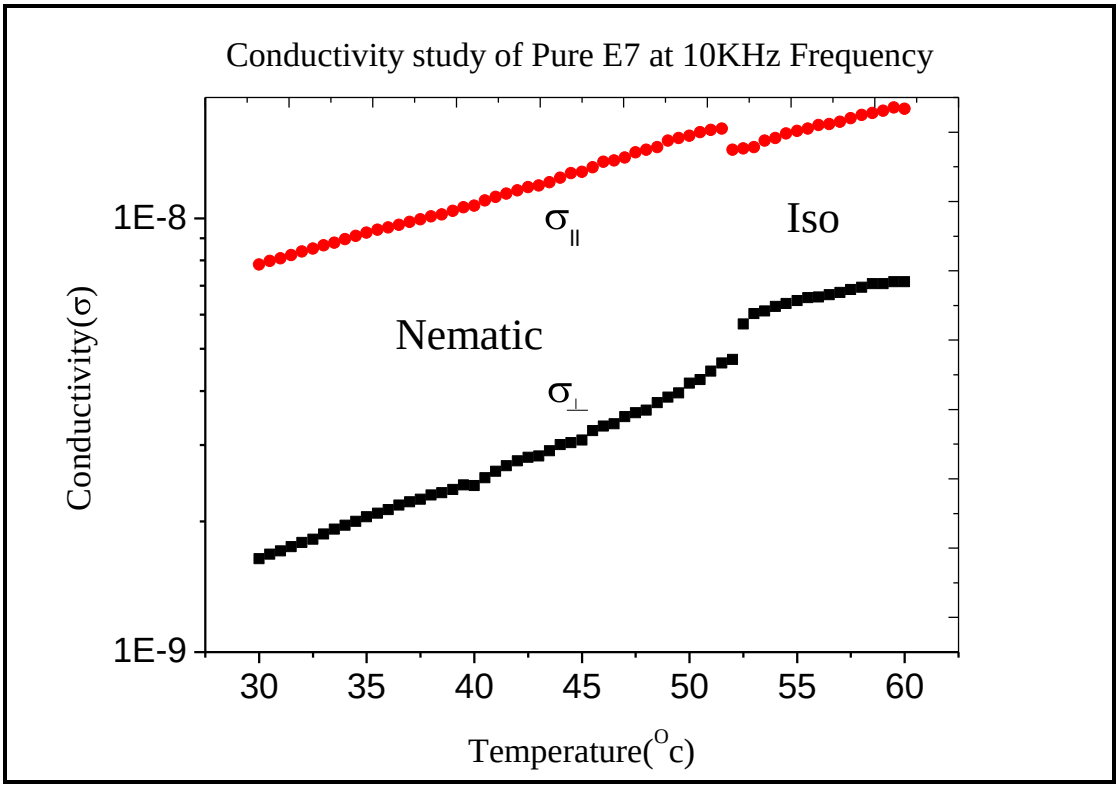

Fig 2.25: Variation of Conductivity as function of temperature for pure E7.

2.3.2.2 Dielectric studies on liquid crystal gold nanocomposites

For our present study we are using two types of gold nanopentagons with different sizes of 18.35nm, 22.14nm.

DIELECTRIC STUDIES ON E7- GOLD NANOPENTAGONS $C_{0.150}$:

Permittivity studies for E7- $GNPC_{0.150}$ solution:

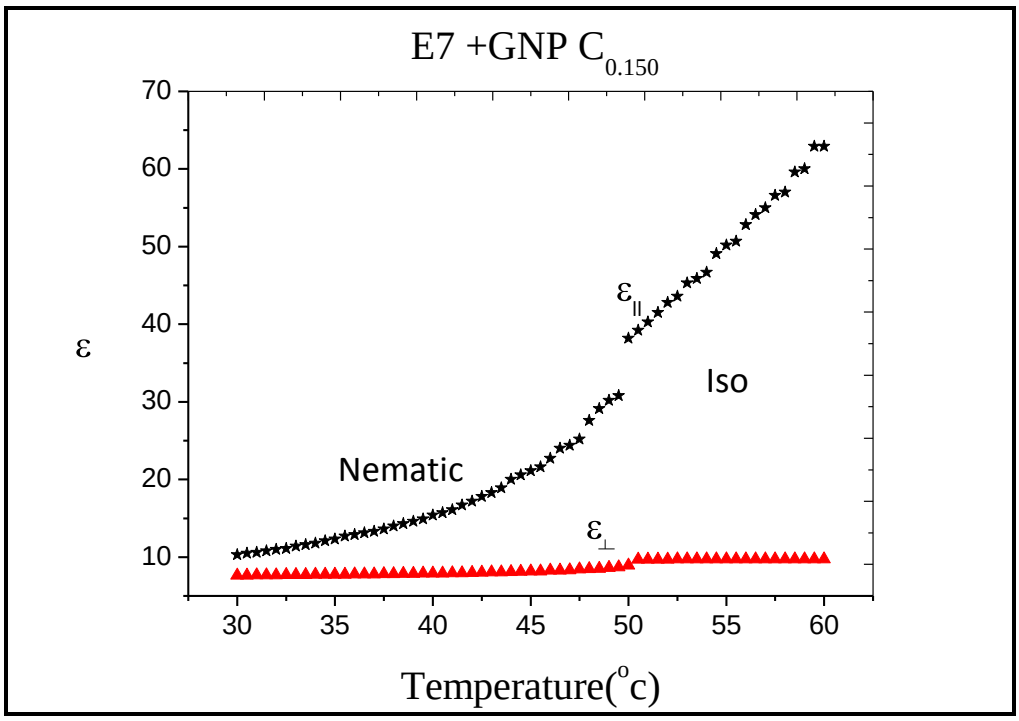

Fig 2.26: Dielectric permittivity for E7- $GNPC_{0.150}$.

Conductivity studies for E7 –GNP $C_{0.150}$ solution:

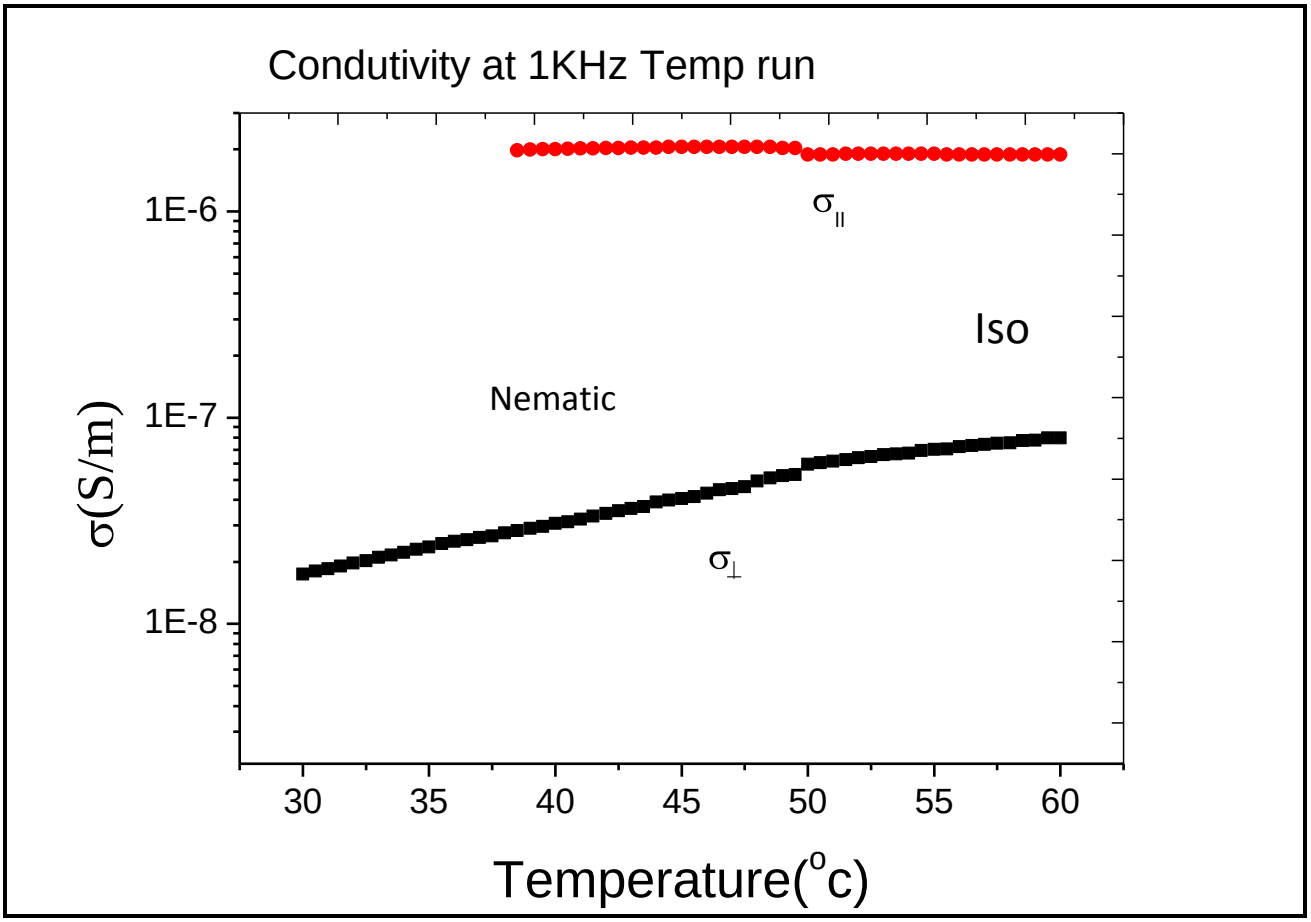

Fig 2.27: Variation of Conductivity as function of temperature for E7-GNP $C_{0.150}$.

For the pure E7 compound the conductivity of the sample is of the order of 10^{-9} but for the LC-nanocomposite the conductivity was increased by ~ hundred times.

GOLD NANOPENTAGONS (SAMPLE 1) WITH E7

Permittivity studies of LC and Gold NanoPentagons (sample 1):

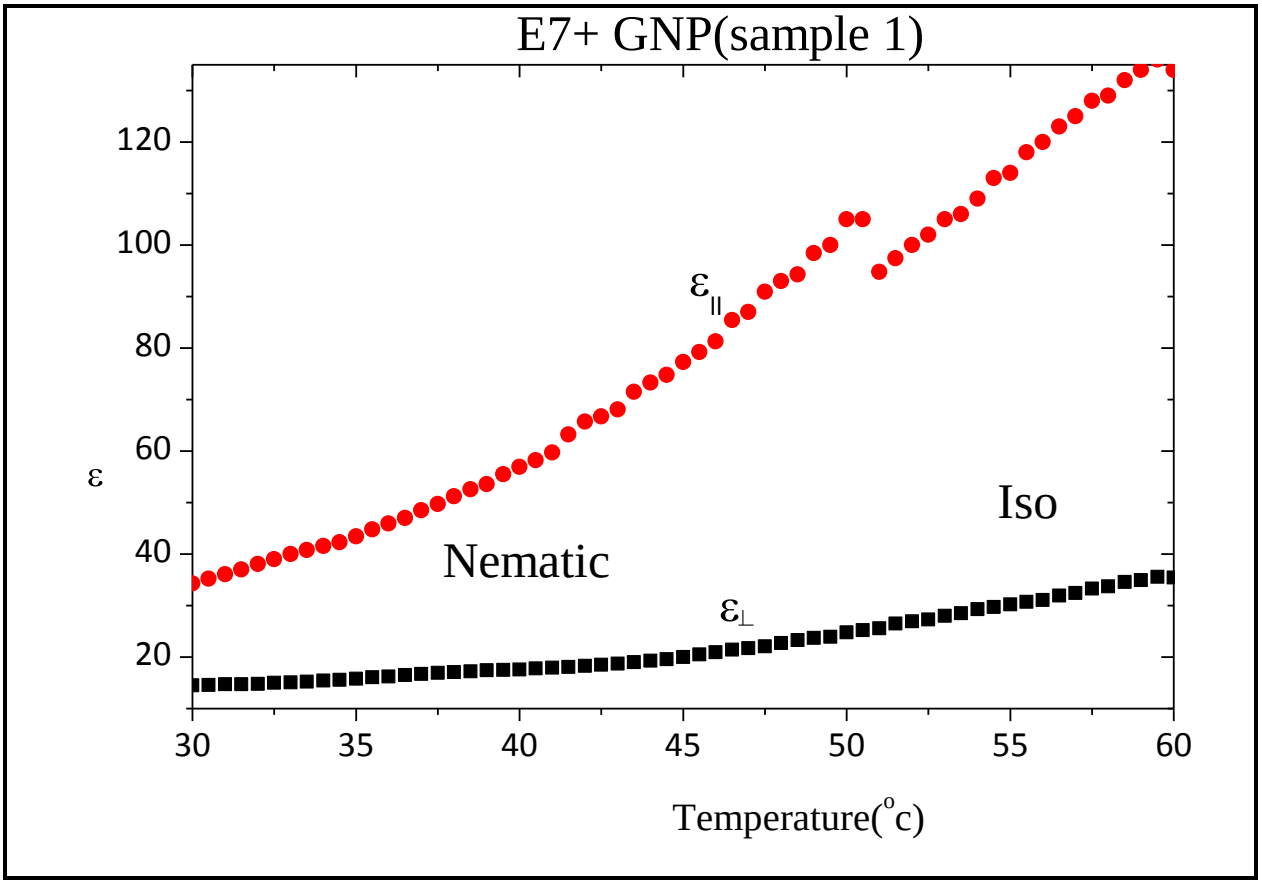

Fig 2.28: Dielectric permittivity as a function of Temperature for E7-GNP (sample 1).

The static permittivity of the sample was measured as a function of temperature. Here the applied input voltage is 0.5V AC and the frequency is 1KHz.

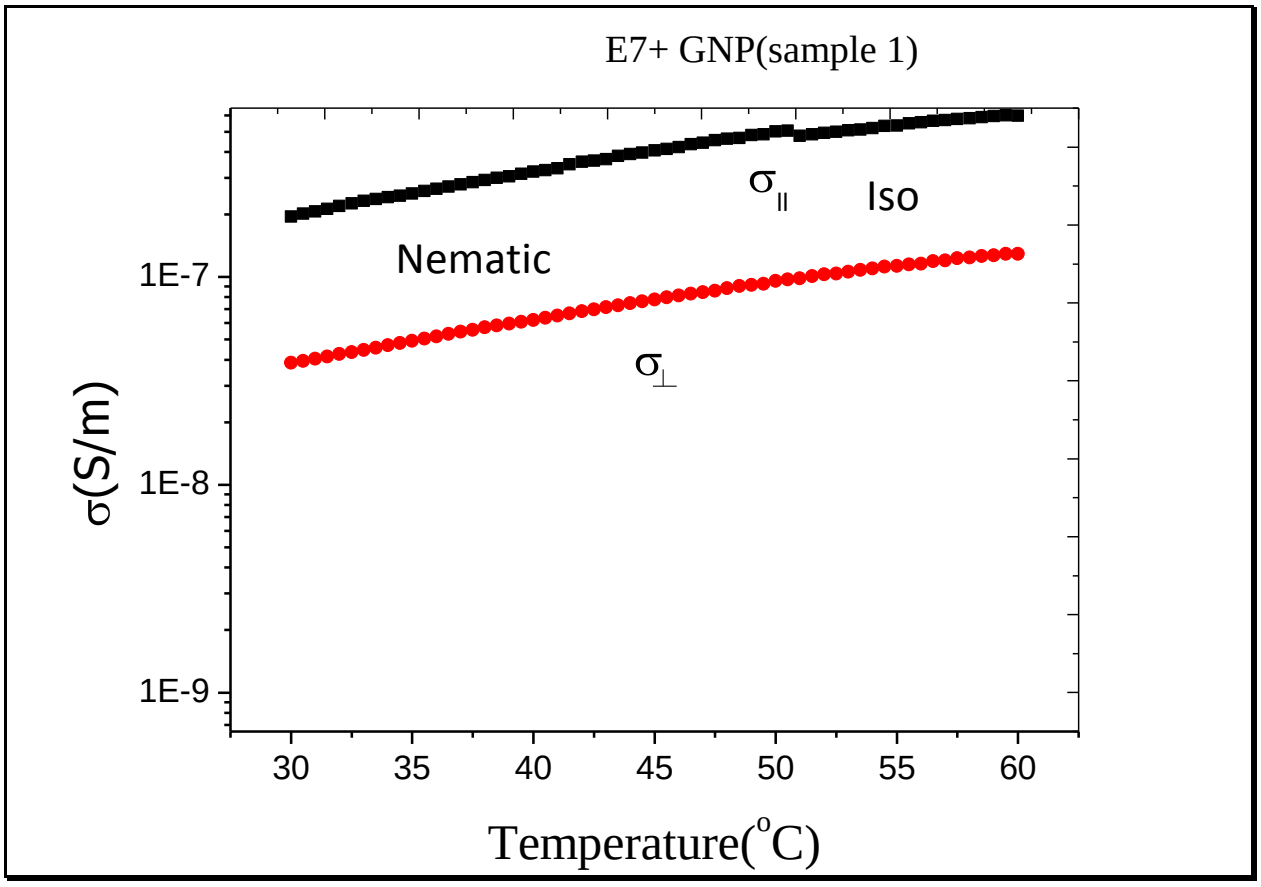

Fig 2.29: Variation of Conductivity as function of temperature for E7-GNP (sample 1).

When the concentration of the metal gold nanopentagons increases the conductivity was increased 100 times compared to the pure E7.

2.4 ELASTIC CONSTANT

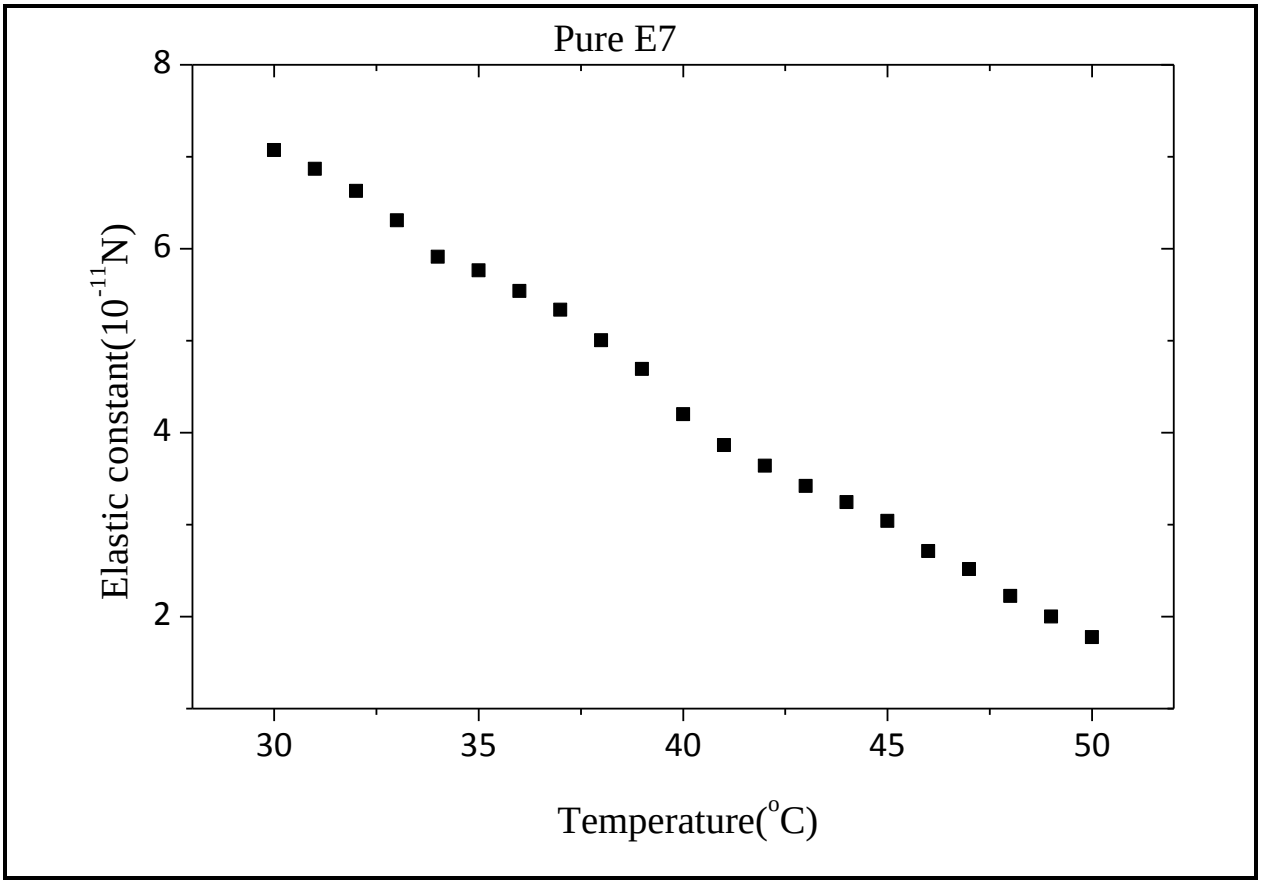

Fig 2.30: The splay elastic constant K_{11} as a function of temperature for pure E7.

The splay elastic constant of the material was increased with the increase in threshold voltage because the elastic constant is directly proportional to the threshold voltage as the temperature decreases. The elastic constant is of the order of 10^{-11} N. The elastic constant of the material was reduced when the temperature will increased. The splay elastic constant was of the order of 10^{-11}N and increased with increase in temperature.

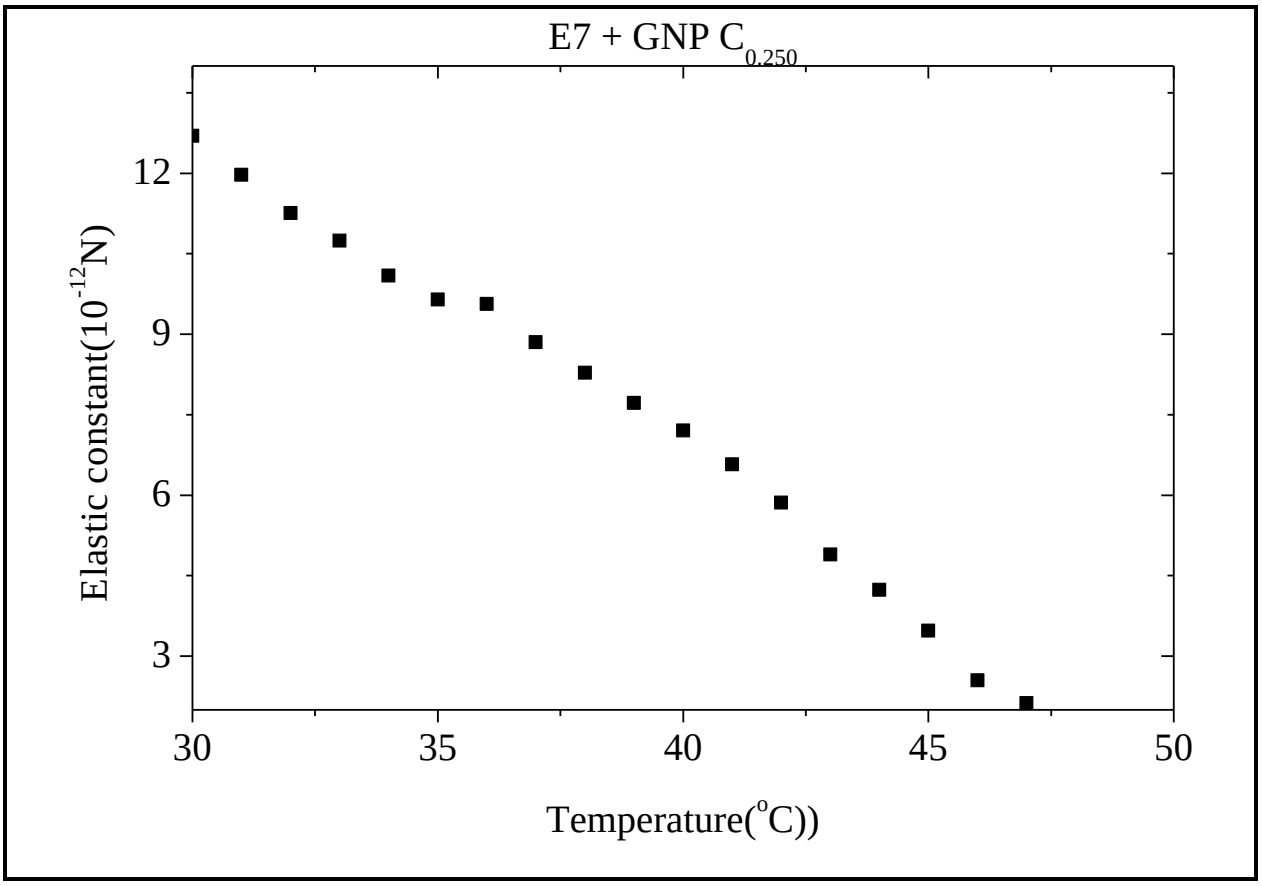

Fig 2.31: The splay elastic constant K_{11} as a function of temperature for E7- GNP $C_{0.250}$.

The splay elastic constant of the composite material was reduced because of the influence of the nanoparticles, compared with the pure LC.

2.5 COMPARISON OF RELAXATION FREQUENCY OF LIQUID CRYSTAL AND LIQUID CRYSTAL NANOCOMPOSITES

Theoretical and experimental studies on dielectric relaxation of heterogeneous dielectric media composed of LC and metal nanoparticles have shown that the relaxation frequency depends on the concentration of nanoparticles (24). Our dielectric results as function of frequency is in general agreement with these results. The relaxation frequency was found to increase with increase in concentration of the nanoparticles.

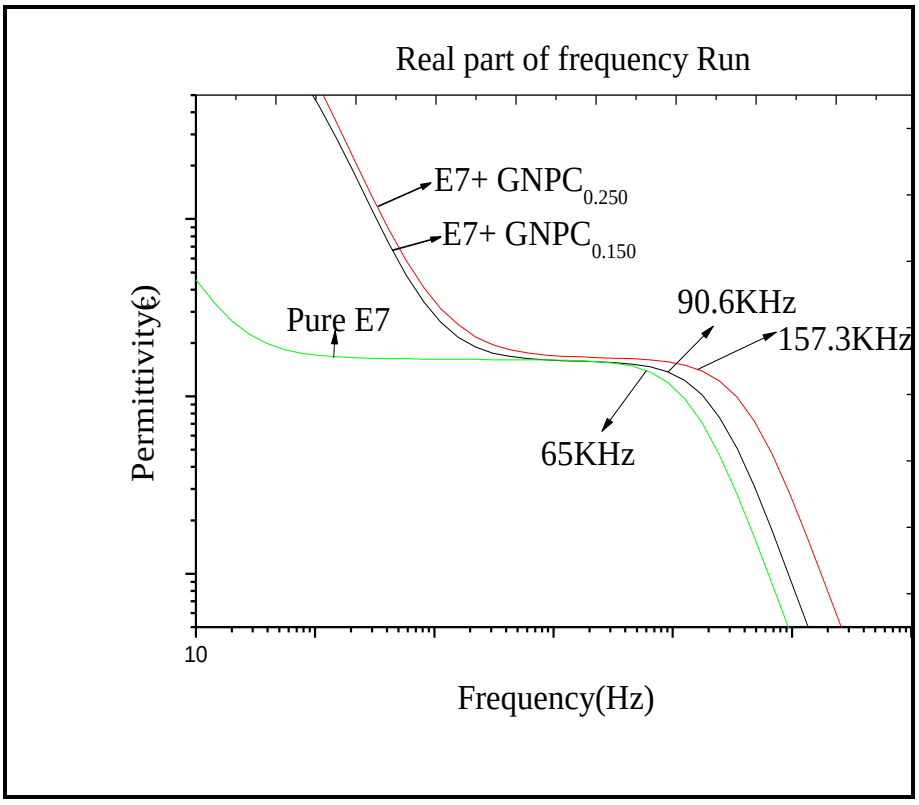

Fig 2.32: Comparison of relaxation frequency of the real part of the permittivity of E7 and E7- nanocomposites.

The frequency dependence of the real part of the permittivity value of the samples E7+ $GNPC_{0.150}$, E7+GNP $C_{0.250}$ of gold nanopentagons was compared with the pure E7 (Fig2.32). The relaxation frequencies for the LC-nanocomposite samples were 157.3KHz for the E7+ GNP $C_{0.250}$ concentration, and 90.6 KHz for E7+ GNP $C_{0.150}$ concentration sample respectively whereas the relaxation frequency for pure E7 was 65KHz. Compared to the pure E7 the relaxation frequency of the composites increased with addition of the nanoparticles.

CHAPTER -III

CONCLUSION

In the presented work, nanoparticles of various shapes were synthesised by changing the concentration of the reducing agents. The nanoparticles were first characterized by using optical absorbance measurement. The shape and size of the nanoparticles were studied using HRTEM. Non-linear optical properties of some of the particles were measured. The nanoparticles were then incorporated into a thermotropic nematic liquid crystal E7 to form LC-nanocomposites. The optical textures and phase stability of the LC-Nanocomposites were first noted using the optical polarizing microscope. The threshold voltage for both the pure LC and the composites was measured using the Freédericksz transition technique. The temperature and frequency dependence of the dielectric permittivity was measured using a high resolution frequency analyser. The conductivity was also obtained using the same instrument. Using the values of the threshold voltage and the permittivity values the elastic constants were obtained. The measurements were carried out for both low and high concentration of nanoparticles of different shapes. A comparison of the properties exhibited by pure LC and the nanocomposites showed that the addition of the nanoparticles definitely has an effect.

CHAPTER -IV

SCOPE OF FUTURE WORK

Liquid crystals play a vital role in display devices. Thermotropic liquid crystals are specially used in electro optic devices like analytical instruments, laptops, calculators, cameras, digital multimeter, thermometer, light emitting diode etc. The reduction of the threshold voltage and increase in dielectric constant observed with the addition of the nanoparticles can be very useful for practical applications. The wavelength of the surface plasmon resonance of such LC nanocomposites can also be tuned and can lead to interesting optical applications.

REFERENCES

1. U.Kreibig, M.Vollmer,(1995) ‘optical properties of metal clusters’, springer- verleg, Berlin.

2. Pierre-Gilles de Gennes, JacquesProst,(1993) ‘The Physics of liquid crystals’, Clarendon press, second edition.

3. S. Chandrasekhar,(1993) ‘Liquid Crystals’, Cambridge University press, Second Edition.

4. Ingo Dierking,(2002) ‘Texture of Liquid crystals’, Wiley-vch.

5. D. Demus, J. Goodby, G.W. Gray,H.-W. Spiess, V Vill,(1999) ‘Physical Properties of Liquid Crystals’, Wiley-Vch.

6. Shin- Tson Wu, Uzi Efron, and LaVerne D.Hess,(1984) ‘Birefringence measurements of liquid crystals’, Applied Optics, 23 (21), 3911-3915.

7. G.Mie,(1908) ‘Contributions to the optics of turbid media, particularly of colloidal metal solutions’, Annalen der physic, 25(3), 377-445.

8. J. Kimling, M. Maier, B. Okenve, V. Kotaidis, H. Ballot, and A. Plech,(2006) ‘Turkevich Method for Gold Nanoparticle Synthesis Revisited’, J. Phys. Chem. B, 110, 15700-15707.

9. Mathias Brust, Merry1 Walker, Donald Bethell, David J. Schiffrin and Robin Whyman, (1994) ‘Synthesis of Thiol-derivatized Gold Nanoparticles in a Two-phase Liquid-Liquid System’, J. Chem. Soc., chem. Commun., 801-802.

10. Jana, N. R.; Gearheart, L.; Murphy, C. J.(2001) ‘Seeding Growth for Size Control of 5-40 nm Diameter Gold Nanoparticles’, Langmuir, 17,6782- 6786.

11. Anand Gole and Catherine J. Murphy,(2004) ‘Seed-Mediated Synthesis of Gold Nanorods: Role of the Size and Nature of the Seed’, Chem. Mater. 16, 3633-3640.

12. Sandeep Kumar, Satanu K.Pal, V.Lakshminarayanan,(2005) ‘Discotic decorated gold nanoparticles’, Mol. Cryst. Liq. Cryst, 434, 579-586.

13. R. Pratibha, K. Park, I. I. Smalyukh and W. Park,(2009) ‘Tunable optical metamaterial based on liquid crystal-gold nanosphere composite’, Optics Express 17(22) , 19459-19469.

14. R. Pratibha, W. Park, and I. I. Smalyukh,(2010) ‘Colloidal gold nanosphere dispersions in smectic liquid crystals and thin nanoparticle-decorated smectic films’, Journal of Applied Physics 107, 063511.

15. G. P. Verma,(2001) ‘Fundamentals of Histology’, New Age International.

16. Nina Berova, Kōji Nakanishi,(2000) ‘Circular dichroism: principles and applications’, Wiley-VCH.

17. Robert W. Kelsall, Ian W. Hamley, Mark Geoghegan,(2005) ‘Nanoscale Science and Technology’, John Wiley & Sons Ltd.

18. Laud, B.B, (1993) ‘Laser and nonlinear optics’, 2nd Ed, Wiley Eastern Ltd.

19. M. Sheik-Bahae et.al,(1990) ‘Sensitive measurement of optical nonlinearities using a single beam’, IEEE J. Quantum Electron., 26, 760-769.

20. Colleen L. Nehl, Hongwei Liao,Jason H. Hafner,(2006) ‘Optical Properties of Star-Shaped Gold Nanoparticles’, Nano Lett., 6(4), 683- 688.

21. Linfeng gou and Catherine J. Murphy, (2005) ‘Fine tuning shape of gold nanorods’, chem. Mater. 17, 3668-3672.

22. Dongheun Kim, Jinhwa Heo, Minjung Kim, Young Wook Lee, Sang Woo Han,(2009) ‘Size-controlled synthesis of monodisperse gold nanooctahedrons and theirsurface-enhanced Raman scattering properties’, Chemical Physics Letters 468, 245–248.

23. Kou et al,(2006) ‘Growth of gold nanorods and bipyramids using CTEAB surfactant’, J. Phys. Chem, B, 110(33), 16377-16383.

24. Kobayashi et al.,(2006) ‘Dielectric spectroscopy of metal nanoparticle doped liquid crystal displays exhibiting frequency modulation response’, Journal of display technology, 2(2), 121-129.